8-1-1989

Modification of structurally different polymers downstream of a microwave plasma

J. Patrick Kusior

MODIFICATION OF STRUCTURALLY DIFFERENT POLYMERS DOWNSTREAM OF A MICROWAVE PLASMA

J. PATRICK KUSIOR

August, 1989

THESIS

SUBMITTED IN PARTIAL FULFILLMENT OF THE REQUIREMENTS FOR THE DEGREE OF MASTER OF SCIENCE

APPROVED:

Vladimir Vukakovic
Project Advisor

Gerald A. Lakaez
Chemistry Department Head and Project Advisor

Robert A. Clark
Materials Science and Engineering and Project Advisor

Robert A. Clark
Director, Materials Science and Engineering

Library

Rochester Institute of Technology
Rochester, New York 14623
Materials Science and Engineering

MODIFICATION OF STRUCTURALLY DIFFERENT POLYMERS
DOWNSTREAM OF A MICROWAVE PLASMA

August, 1989

TABLE OF CONTENTS

FIGURE CAPTIONS

Note: Throughout the text the phrase "spin coated PI wafer" is used. This phrase refers to a silicon wafer that has been spin coated with polyamic acid. To cure the polyamic acid, the silicon wafer was placed in an oven. The curing process produces a silicon wafer with a top layer of polyimide.

LIST OF TABLES

ACKNOWLEDGEMENTS

I would like to thank my Mother and family for instilling in me the value of an education.

Many people have contributed, in one form or another, to the completion of this thesis. I thank my three primary advisors. They are: Dr. Vladimir Vukanovic, Dr. Gerald Takacs and Dr. Robert Clark.

I thank the outstanding people that I worked with at the RIT Plasma Lab. They are: Dan Tracy, Mark Heitz, Dr. David Harding, Kevin Gillman, Jay Pinkes, Matt Freeman, Violeta Mugica and Dr. Yu.

I appreciate the help that Norene Chesterton, Debbie Kipler and her husband Mike Koch have given me with the word processing of this thesis.

For making life outside of the laboratory very enjoyable; I thank a special friend, Sharon Mazurek.

1.0 INTRODUCTION

Since the mid 1960's there have been numerous papers published on the modification of organic polymers in a pure oxygen or oxygen-fluorocarbon plasma. In terms of this thesis, chemical modification occurs when a polymer is either passivated (fluorinated) or etched. Many parameters influence the degree to which a polymer is modified downstream of a microwave (MW) plasma. Some of the parameters include: substrate temperature, MW power, gas feed composition, chamber pressure and total gas flow rate; the latter two determine the gas flow velocity. One of the more important parameters, in the case of polyimide (PI), which influences etching, is the [O]/[F] ratio. That is, the ratio between the atomic oxygen concentration and the atomic fluorine concentration. [1,2,3]

A topic of increasing importance is the degree to which a polymer is susceptible to modification, by a plasma, according to the structure of the polymer. For example, is a saturated polymer more likely to undergo etching or passivation compared to an unsaturated polymer? In addition, the plasma fluorination of structurally different polymers and the degree to which fluorination occurs has not been widely established.

In 1965, Hansen, Pascale, De Benedictics and Rentzepis [4] performed weight loss experiments on 36 structurally different polymers. The experiments were done to investigate the effect of plasma generated atomic oxygen on the polymers. All the polymers tested underwent rapid reactions at the polymer film - plasma interface. Highly branched polymers such as polypropylene and polymers having ether linkages such as polymers of formaldehyde were most readily etched. Polymers which were the most resistant to reactions with atomic oxygen were the perfluorinated polymers, highly aromatic polymers and sulfur-vulcanized rubbers.

Taylor and Wolf [5] examined the relative rates of polymer removal in an oxygen plasma for 40 polymers. The removal rates were retarded if the polymer contained either one of the following: strong backbone bonds, polar functional groups, metallic bonds or an aromatic structure. Weak bonds attached directly to the chain greatly accelerated removal; while weak bonds not attached to the polymer backbone had little effect. It was also reported that all the polymers showed increased removal rates if a mixture of CF4 and O2 was used. The addition of CF4produces F atoms which can react with the polymer surface.

A theory concerning the role of atomic fluorine in relation to the plasma etching of structurally different polymers has been proposed by Cain, Egitto and Emmi. [6] The mechanisms of etching were inferred theoretically from a molecular orbital study. This theory is discussed in more detail in section 4.0.1.

To date, three methods have been proposed as to how F atoms enhance etching. They are: hydrogen abstraction [7], addition to olefinic groups [8] and indiscriminant abstraction of atoms other than hydrogen. [9] An excess of F atoms will inhibit etching through competition with O atoms at sites on the polymer surface. [2] The excess fluorine results in the formation of CF2 type bonding. [1,2,10,11]

This work examines the experimental factors which influence the surface modifications and bulk modifications of structurally different organic polymers. Surface analysis of the polymers was performed by scanning electron microscopy (SEM), x-ray photoelectron spectroscopy (XPS) and contact angle measurements. Gravimetric analysis was used to investigate bulk modifications. Etch rates of the polymers were determined by laser interferometry and weight loss measurements.

The remaining portion of the introduction is divided into five sections. Sections 1.1 and 1.2 give a brief description of the etching and fluorination processes. The next section discusses some of the parameters that influence

the modification of a polymer which is exposed downstream of a MW plasma. Section 1.4 describes the chemistry of a CF4-O2 plasma. Section 1.5 looks at the production of atomic oxygen in a MW plasma and the last section focuses on the reactions of the plasma produced gas species at saturated and unsaturated polymer surfaces.

1.1 Etching

In plasma etching, the starting material often contains a relatively inert gas. A low pressure, LP, glow discharge is established by subjecting the inert gas to a source of energy; be it a microwave generator or a radio-frequency generator. Reactive gas species are produced by the LP glow discharge. Etching occurs when the reactive species react with a thin film to form a volatile product that is pumped away. [12-14] The rate of etching has been suggested to be dependent on either the rate of active species arriving at the polymer surface [15] or the removal rate of the volatile products from the polymer surface. [16]

An important advantage of plasma etching (dry etching) over wet etching is that dry etching can be anisotropic (directional). Other advantages are: operator safety, increased cleanliness, adaptability to automation and a reduced ecological impact. [17]

A substrate undergoing etching can be in either of two locations during an experiment. It can be in the plasma (discharge zone) or it can be removed from the plasma. The term downstream plasma etching refers to the latter case. Substrates placed directly in the discharge zone can be etched anisotropically because the plasma is at a greater positive electrical potential compared to the surfaces with which it is in contact. The end result is that ions are accelerated along field lines running perpendicular to these surfaces. [18] Substrates downstream of a plasma generally undergo isotropic etching. Two advantages of having the substrate downstream of a plasma are: easier substrate temperature control and no ion bombardment induced damages at the polymer surface. [18] If the sample is removed from the plasma, it will also be subjected to fewer electrons and photons.

1.2 Fluorination

Exposure of polyimide (PI) downstream of a MW plasma, with a high concentration of CF4 in the gas feed, leads to the formation of a fluorinated layer at the PI surface. [19] The mechanism leading to this fluorinated layer is not well established, but it could be similar to the proposed fluorination pathway of a saturated polymer (Figure 1). Polymers which are heavily fluorinated are resistant to etching downstream of a MW plasma even if the plasma has an

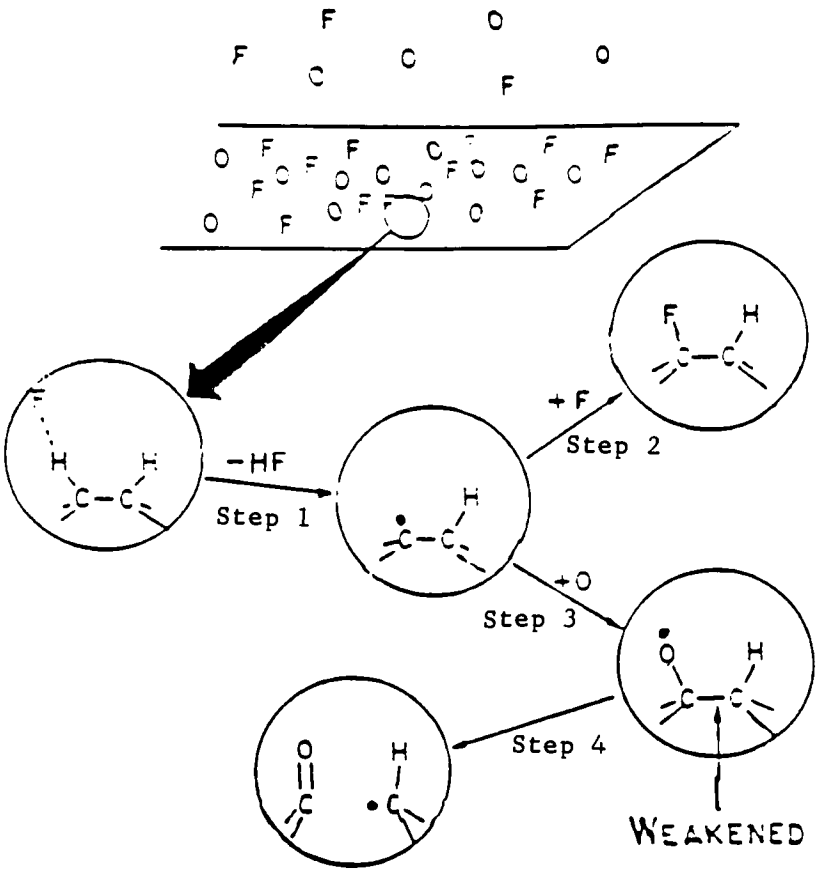

Figure 1. Reaction scheme of F atoms reacting at a saturated polymer surface.

abundance of O atoms. [12,19,20] The enhanced etch resistance of plasma-fluorinated PI has been attributed to extensive formation of CF2 type structures on the PI surface. [22] The depth of the fluorinated layer is dependent on the following: time of exposure to a F-rich plasma [12,20,21], the chemical composition of the polymer [12,20], the plasma parameters and the type of etching apparatus. [12,20,21]

SEM (scanning electron microscope) micrographs show that the fluorination of spin coated polyimide (PI) does not alter the initially smooth surface (Figure 2). XPS (X-ray photoelectron spectroscopy) studies by Matienzo, Emmi, Egitto, Van Hart, Vukanovic and Takacs [22] reveal that the fluorinated surface of PI reaches a constant composition of 56% F, 35% C, 3% N and 17.2% O after an approximate 10 minute exposure time downstream of a microwave plasma (Figure 3). The percent composition for untreated polyimide is 75.9% C, 6.9% N, 17.2% O. [19]

Rutherford back scattering (RBS) has been used [22] to determine the depth of fluorination. For an exposure time of 1.5 to 10 minutes, the depth of fluorination increased linearly. The depth profile reached a maximum of 600 A after a 30 minute exposure time. The thin film was rich in fluorine up to a depth of 200 A.

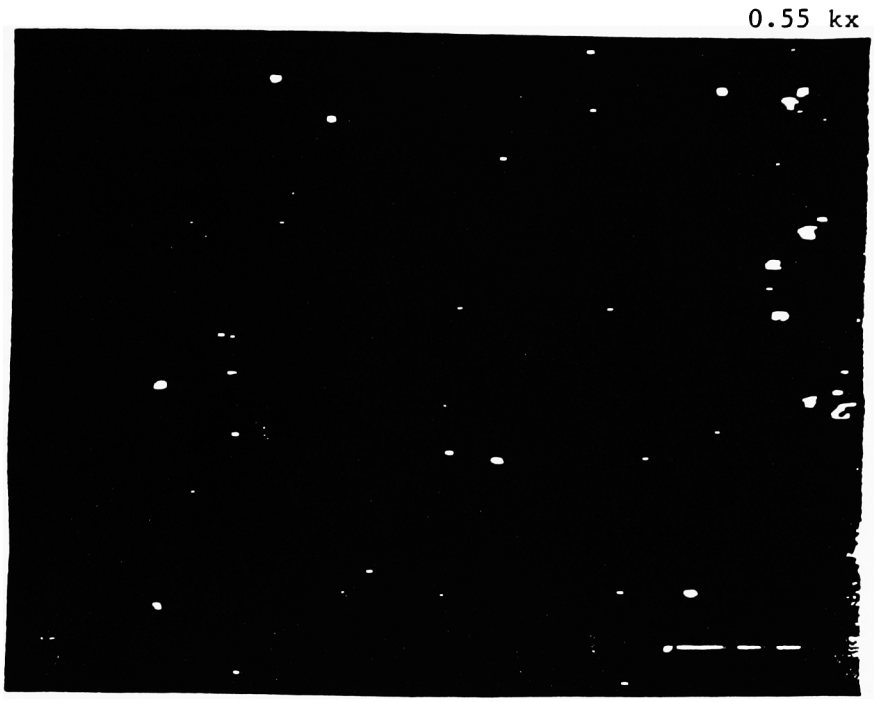

Figure 2. Electron micrograph of a spin coated polyimide wafer that was fluorinated for 130 minutes.

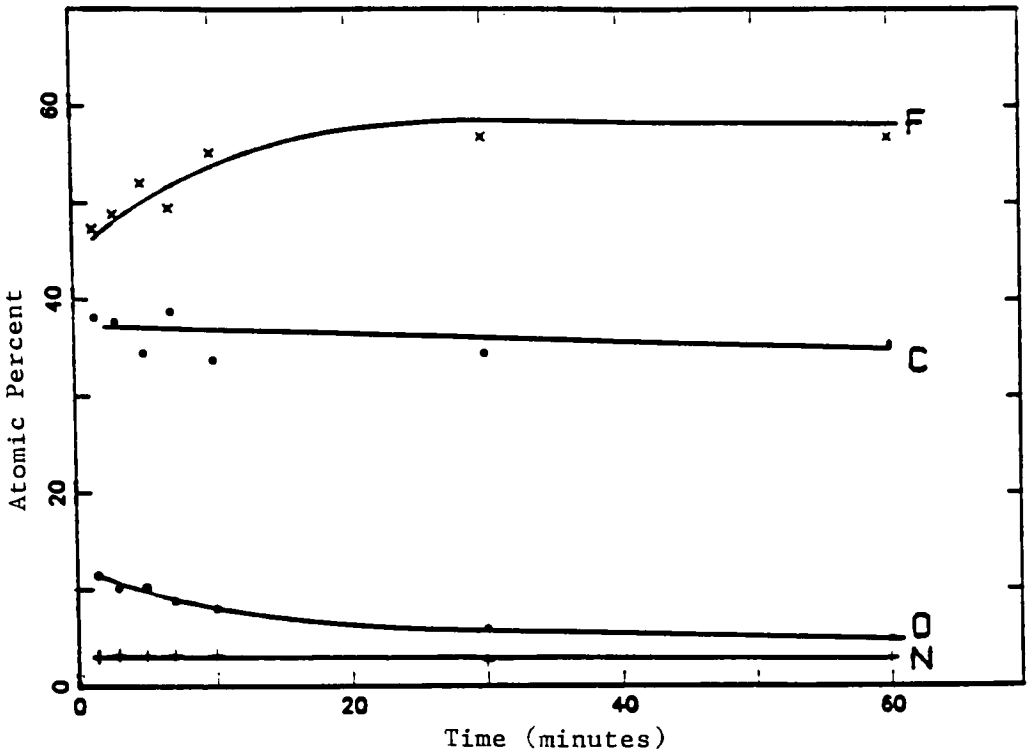

Figure 3. Exposure time of a spin coated PI sample to a fluorine-rich microwave plasma.

1.3 Parameters Which Influence Plasma Modification of Polymers

1.3.1 Temperature

For the case of PI, etch rate increases as temperature increases (Figure 4). [23] The temperature dependence is normally described in terms of the activation energy. The activation energy can be thought of as a "barrier" to chemical reactions or the critical energy that molecules or atoms must aquire before they can react. [18]

1.3.2 Microwave Power

An increase in MW power will result in a higher etch rate. For an O2-CF4 plasma, increased MW power enhances the dissociation of molecular oxygen and carbon tetrafluoride. As a result, more reactive gas species are produced; that is, more CFx ($x < 4$) and atomic oxygen. [23] The chemistry that occurs in the gas phase is discussed in section 1.4.

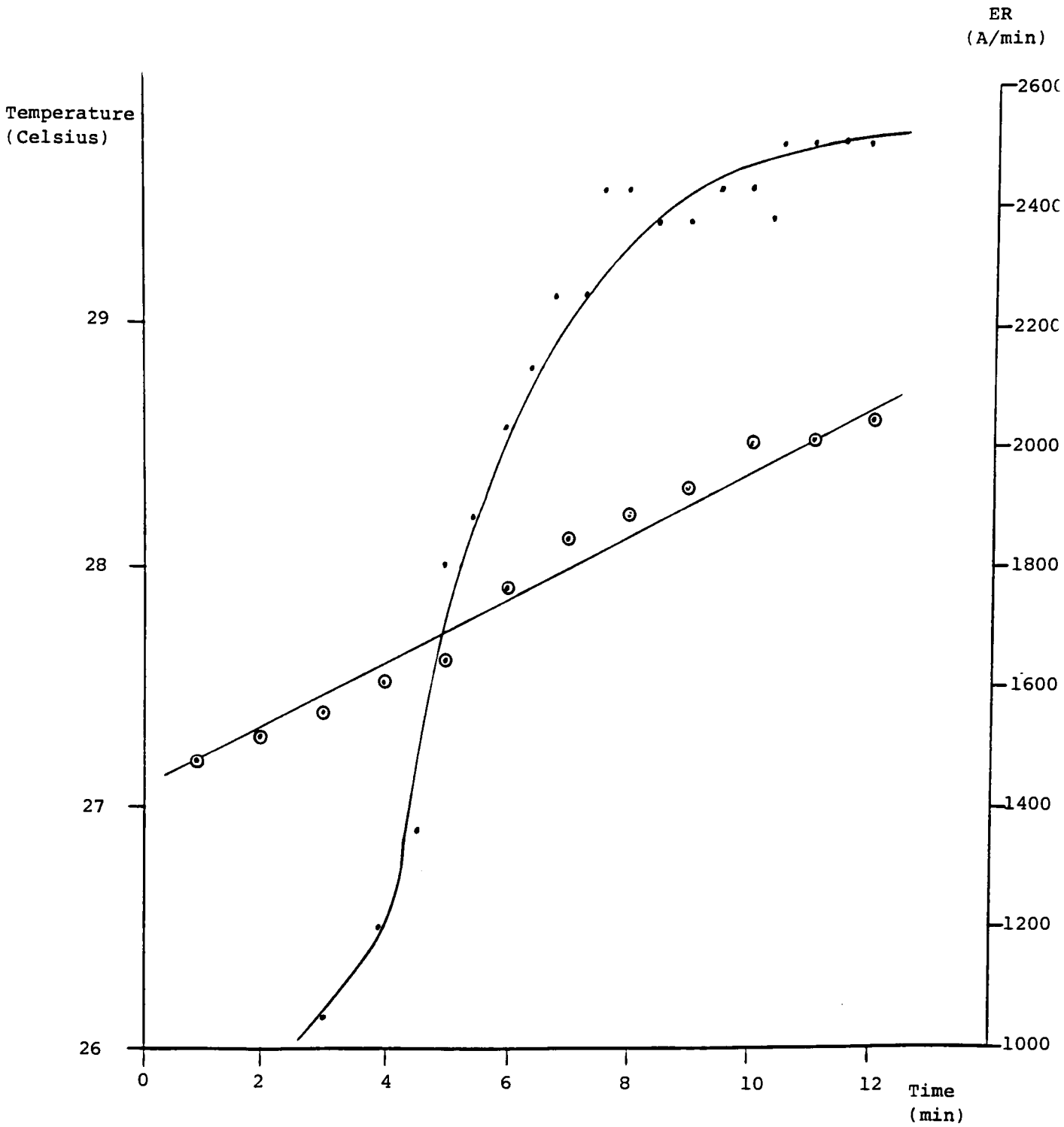

Figure 4. Graph of the temperature vs. time and etch rate vs. time for a spin coated PI sample.

1.3.3 Gas Composition

Carbon tetrafluoride, CF4, is the gas most commonly added to an oxygen plasma in order to enhance the generation of atomic oxygen, thereby enhancing the polymer etch rate. Polymer etch rates are also increased because the addition of F atoms lowers the activation energy associated with the etching of organic polymers. [24] The increase in O atom production is probably due to changes in the electron density and energy distribution in the plasma and not due to free radical reactions. [18]

For CF4-rich plasmas, the addition of molecular oxygen increases the F atom concentration. The increase is due to reactions between O atoms and the dissociated products of CF4 [25-27] or the reaction between electronically excited metastable oxygen molecules and CF4. [28] F atom production is important because the F atoms can abstract hydrogen atoms from the polymer [7]. This creates radical sites on the polymer surface which readily undergo reactions with O atoms.

1.3.4 Residence Time

The slower the flow rate the longer a gas molecule will reside in the MW cavity. The time of residency of the gas molecule in the MW cavity is known as the residence or retention time and is given by:

$$T = L / v \qquad (1)$$

where T is the time in minutes, L is the length of the MW cavity in centimeters and v is the gas flow velocity in standard cubic centimeters per minute. [29]

1.3.5 Gas Flow Velocity

Total gas flow rate and chamber pressure are two parameters which are used to determine the gas flow velocity, v. The equation for v is given below:

$$v = FR \times (760/PR) \times (T/273) \times (1/\pi r^2) \qquad (2)$$

where FR is the total gas flow rate. PR is the reactor chamber pressure. T is the temperature of the gases in Kelvin and r is the tube radius. For the 5-way cross (See section 2.1), r was approximated to be 10 cm. v is proportional to FR and inversely proportional to PR. [23]

Reactive gas species generated in the MW cavity take less time to reach the substrate at higher total gas flow rates and lower reactor pressures. [23] A higher v delivers more plasma produced gas species to the polymer surface per unit time. It also decreases the gas species chance of recombination by homogeneous (gas-phase) or heterogeneous (recombination on the chamber walls) processes. A linear dependency was observed for the etch rate of spin coated polyimide samples on v downstream of a microwave plasma containing 75% O2, 20% CF4 and 5% Ar. [18]

1.3.6 Optical Emission Spectroscopy and the [O]/[F] Ratio

The oxygen-to-fluorine atomic concentration ratio in the plasma is directly proportional to the ratio of intensities of spectral emission lines at 844.6 nm for atomic oxygen and 703.7 nm for atomic fluorine. [6] Optical emission spectroscopy measures the relative number densities of gas species in a plasma [18] and by doing so, it provides a way to obtain the [O]/[F] ratio. As stated previously, there is

an optimum [O]/[F] ratio at which maximum etching occurs. The value of the ratio changes for different polymers and is a function of the chemical properties of the polymer being etched. [29]

If small amounts of CF4 are added to an O2 plasma, greater emission intensities will occur. A higher electron energy distribution function, EEDF, with a higher population of high energy electrons and/or a higher electron density in the plasma can be inferred from the greater emission intensities. [18] If one wishes to increase the number of electron induced dissociations in an O2 or CF4 plasma, then the addition of small amounts of CF4 or O2 , respectively, to these plasmas will help achieve this goal.

When the condition of the plasma changes, there is an accompanying change in the excitation efficiency of the plasma. To compensate for this change, all emission intensities of the gases of interest are normalized to an emission intensity of a spectral line from an inert gas. [30] This technique is known as optical emission actinometry.

For O2-CF4 plasmas, the inert gas most commonly used to normalize atomic oxygen (844.6 nm) and atomic fluorine (703.7 nm) is argon. Ar is used because its emission line occurs at 750.4 nm. This line is used because it is nearly equal in intensity to both the atomic oxygen and fluorine lines. In order for actinometry to be accurate and/or valid, the actinometer gas and the species of interest must both

emit from excited states resulting from collisions with electrons. [18]

1.4 Chemistry of the CF4-O2 Plasma

A model of the chemical processes occurring in a CF4-O2 discharge has been developed by Plumb and Ryan. [31] Rate coefficients were either calculated by the authors or were obtained from the literature for 49 possible reactions which occurred in a MW glow discharge at a pressure of 0.5 Torr. Thirteen of the reactions are considered to be the most prominent. Five of the reactions are electron induced (primary) and the other eight are free radical reactions (secondary) (Refer to Table 1).

The chemistry of the CF4-O2 discharge is summarized by the flow chart shown in Figure 5. The following is a brief description of the Plumb and Ryan model. At high molecular oxygen concentrations, [O2], in the plasma, CF2 produced by the electron induced dissociation of CF4 will react almost entirely with O atoms. The product of this reaction, COF, will rapidly react with atomic oxygen to form CO2 and F atoms (See reaction 9 in Table 1). At long retention times, the CO2 produced in this step will dissociate into CO by reaction 12. CO in turn reacts with atomic fluorine to produce COF which is recycled to produce CO2. Downstream of the plasma, dissociation of CO2 doesn't occur because there

Table 1. Reaction set of the most prominent reactions occurring in an O_2-CF_4 MW plasma.

Reaction Number	Reaction
1	$CF_4 \xrightarrow{e} CF_3 + F$
2	$CF_4 \xrightarrow{e} CF_2 + 2F$
3	$CF_3 + F \xrightarrow{M} CF_4$
4	$CF_2 + F \xrightarrow{M} CF_3$
5	$O_2 \xrightarrow{e} O + O$
6	$CF_3 + O \rightarrow COF_2 + F$
7	$CF_2 + O \rightarrow COF + F$
8	$CF_2 + O \rightarrow CO + 2F$
9	$COF + O \rightarrow CO_2 + F$
10	$COF + F \xrightarrow{M} COF_2$
11	$COF_2 \xrightarrow{e} COF + F$
12	$CO_2 \xrightarrow{e} CO + O$
13	$F + CO \xrightarrow{M} COF$

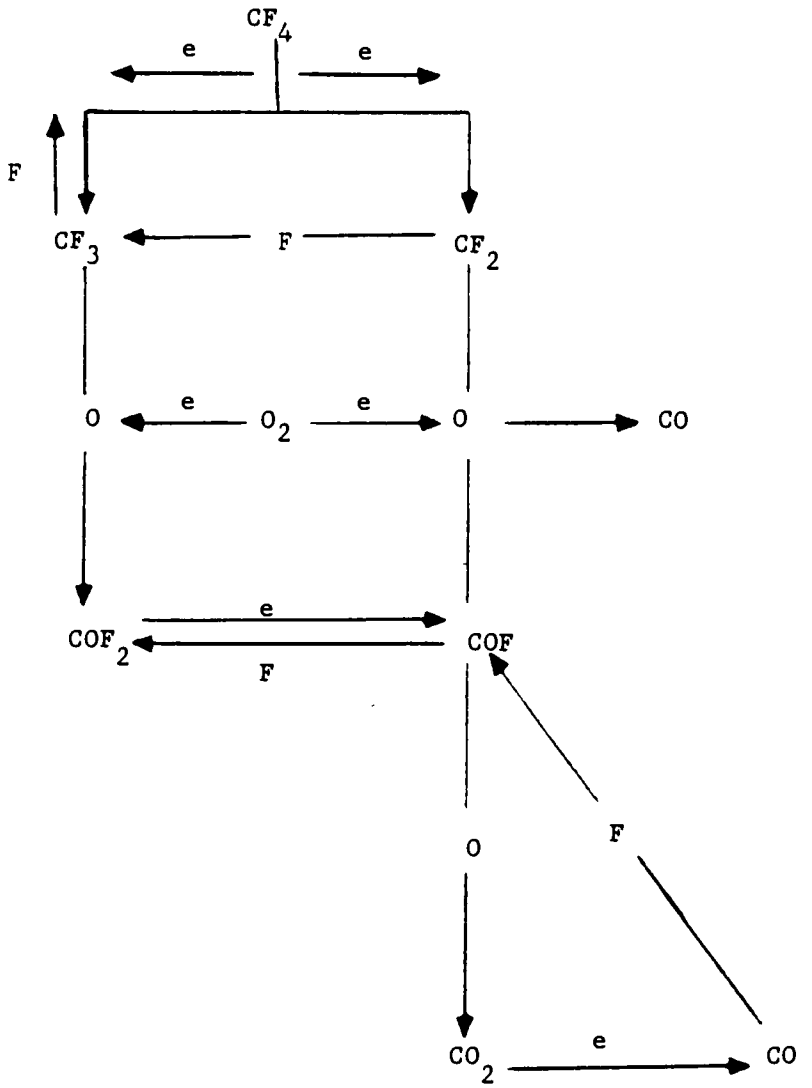

Figure 5. Flow chart of the reactions occurring in Table 1.

are no electrons present. As a result, [CO2] increases while [CO] decreases.

CF2 produced by the dissociation of CF4 will react with atomic oxygen to produce COF (reaction 7). Since the dissociation of COF2 is electron induced, longer retention times will yield more product, COF + F (reaction 11), which will eventually lead to more CO2 and CO.

Plumb and Ryan have concluded that high F atom (low O atom) containing plasmas have COF2 as the principal product whereas high O atom containing plasmas have CO2 as the principal product.

Since five of the seven fluorine atom producing reactions are dependent on atomic oxygen, it is worth while to investigate how the production of O atoms can be enhanced.

1.5 Atomic Oxygen Production

The production of atomic oxygen in a plasma is dominated by electron induced dissociations of molecular oxygen reactions. Some of the more important reactions between oxygen (molecular, atomic and ionized) and electrons are shown in Figure 6. Reactions 15 and 16 probably proceed via an intermediate O_2^* (Figure 7). Reaction 21 (Figure 7) produces two ground state O atoms, while reaction 22

$$e + O_2 \rightarrow O_2^* + e \quad (14)$$

$$\rightarrow 2O + e \quad (15)$$

$$\rightarrow O^* + O + e \quad (16)$$

$$\rightarrow O_2^- + 2e \quad (17)$$

$$\rightarrow (O_2^-)^* + 2e \quad (18)$$

$$e + O \rightarrow O^* + e \quad (19)$$

$$e + O_2^- \rightarrow (O_2^-)^* + e. \quad (20)$$

Figure 6. Electron reactions, occurring in a microwave plasma, with molecular oxygen, atomic oxygen and excited state molecular oxygen.

$$e + O_2 \rightarrow O_2^*(A^3\Sigma_u^+) \rightarrow O(^3P) + O(^3P) + e \quad (21)$$

$$e + O_2 \rightarrow O_2^*(B^3\Sigma_u^-) \rightarrow O(^3P) + O(^1D) + e \quad (22)$$

Figure 7. Electron induced dissociation of molecular oxygen via two different excited state molecular oxygen intermediates.

produces one ground state O atom and an excited state (1D) O atom.

The dissociation of molecular oxygen can be enhanced by changing the electron energy distribution function, EEDF. A modification of the EEDF which increases the number density of electrons that possess the energy required to dissociate molecular oxygen will increase the production of atomic oxygen.

1.6 Reactions at Saturated and Unsaturated Polymer Surfaces

As stated previously, the etching of a polymer can be enhanced by: indiscriminant abstraction [9], fluorine abstraction of hydrogen [7] or fluorine addition to olefinic groups. [8] Hydrogen abstraction, and the steps that occur afterwards, from a saturated polymer by fluorine is shown in Figure 1. Step 1 is the abstraction of hydrogen to form a radical site. For a fluorine-rich plasma, fluorine incorporates itself into the polymer network. This leads to the passivation of a polymer (step 2). For an oxygen-rich plasma, oxygen forms a bond at the radical site which weakens the adjacent C-C bond (step 3). Step 4 is an alkoxy degradation which breaks the C-C bond. For a saturated polymer, steps 1, 3 and 4 are the proposed reactions in the etching process: steps 1 and 2 represent the passivation process. [18]

The etching of unsaturated polymers is initiated most probably by the addition of F or O atoms to a C=C double bond. Once this occurs, the double bond is decreased to a C-C single bond. Etching or passivation can now proceed through this saturated intermediate. [18]

In summary, the initiating step for a saturated polymer is H abstraction by F or O atoms and it is F or O atom addition across a C=C double bond for an unsaturated polymer.

2.0 EXPERIMENTAL

2.1 Microwave Plasma Modification System

The microwave system was designed and constructed by Edward A. Matuszak [23] for his 1986 graduate thesis work. The system, as it was used for the results of this thesis, consisted of 12 components: 1) 5-way Pyrex 7740 cross, 2) quartz injector tube, 3) vacuum pump, 4) microwave (MW) source, 5) MW clip-on cavity, 6) gas flow readout unit, 7) mass flow controller, 8) pressure gauges, 9) He-Ne laser, 10) chart recorder, 11) ammeter and 12) photodiode. A schematic of the system is shown in Figure 8. Details about each component are described below.

2.1.1 Reactor Chamber and Injector Tube

The reactor chamber used to investigate the passivation, etching and removal of passivation of structurally different polymers downstream of a MW plasma consisted of a 5-way Pyrex 7740 cross. Each arm has a 4" (10.16 cm) i.d. which extends 7" (17.78 cm) from the center of the cross. The Pyrex cross is situated on a work bench in such a manner that one arm is pointing towards the experimenter, 2 arms are pointing sideways (one to either side) and of the remaining 2 arms; one is extending downward and the other is extending upward (Figure 9).

The ends of the arms are flared with an O-ring groove in the glass. All the arms were sealed at their ends by 1/4" thick aluminum plates. A # 245 Viton O-ring sat firmly between the groove in the arms and a groove in the aluminum plate. This helped achieve a vacuum tight seal. The aluminum plates were held in place against the ends of the cross with metal flanges, inserts, nuts and bolts. [23]

The arm facing the experimenter served as an entrance/exit port for the samples. This arm achieved a vacuum tight seal in the manner described above; however, no flanges, nuts or bolts were used. The aluminum plate was held in place when the reactor chamber was evacuated. The placement and removal of samples during successive runs was

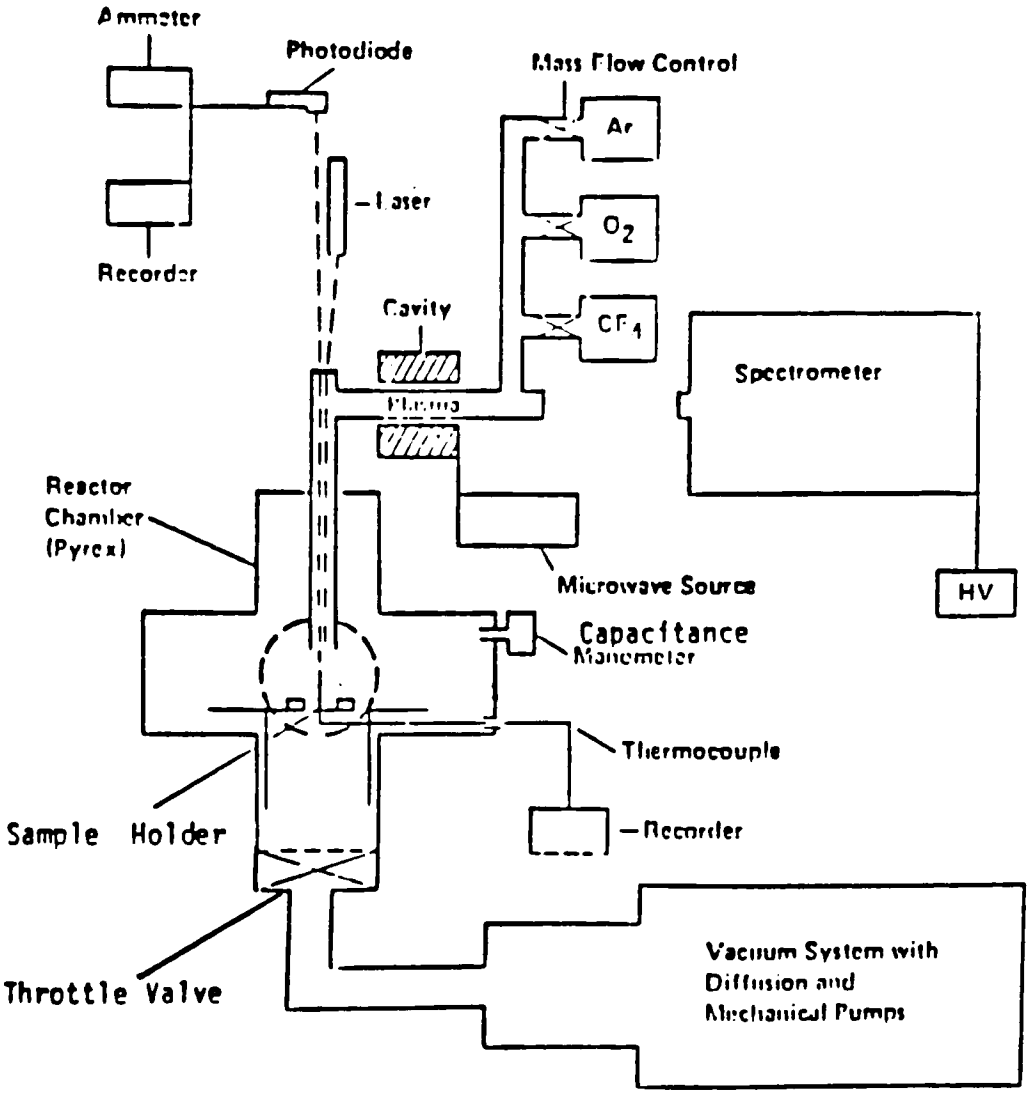

Figure 8. Schematic of the microwave plasma modification apparatus.

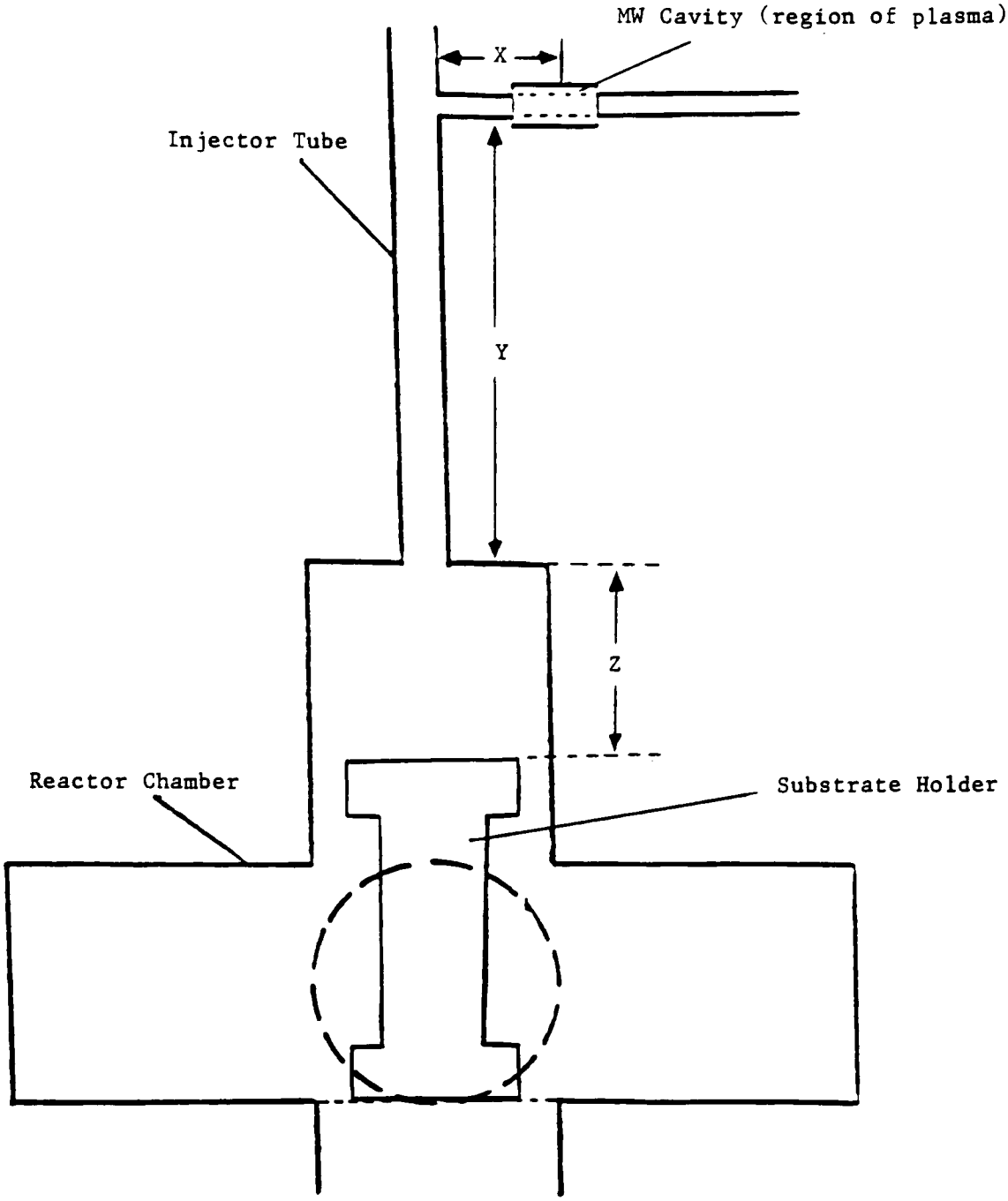

Figure 9. Schematic of the reactor chamber showing the x, y and z distances. x-5.3 cm, y-10cm, z-6.5 cm (with ring substrate holder), z-6.9 cm (without ring substrate holder).

facilitated by not having to bolt an aluminum plate onto the entrance/exit port.

The quartz injector tube was connected to the top aluminum plate via a 1" stainless steel Cajon ultra-torr male connector. The ultra-torr male connector was threaded into the aluminum plate. Teflon tape around the threads and a Viton O-ring provided a vacuum tight seal. The inside of the fitting was bored out in order to allow the quartz tube to pass through and enter into the reactor chamber. The Cajon fitting provided a vacuum tight seal with quick finger-tight assembly. [23] The vast majority of experiments were carried out using a quartz injector tube. However, a few early experiments were performed using a glass injector tube. The change from glass to quartz occurred because quartz reacts less with the gas species produced by the MW plasma. After exposure to a plasma for not more than 12 hours, the glass tube was beginning to show signs that it was being etched. One very noticeable sign was that the tube changed from being clear and transparent to that of being white and translucent. No such change in the quartz injector tube has been observed.

There were two kinds of substrates (samples) which were exposed downstream of the plasma: 1) films and 2) spin coated wafers. The films were: Dupont Kapton H and low density polyethylene (PE). Polyimide (PI), polybutadiene (PB), polyvinyl alcohol (PVA) and polystyrene (PS) were spin coated onto 5.7 cm silicon (Si) wafers. The Kapton H film

(40 micrometers) was placed on an aluminum stud and an aluminum ring was pressed onto the stud. This provided a compression fit for the Kapton H film (Figure 10a). The compression fitting was placed on top of a 13.5 cm tall substrate holder and was held in place by a screw-on cap (Figure 10b). When no experiments with the Kapton film were being performed, the spin coated Si wafers and PE samples were also placed on top of the substrate holder. The screw on cap was used in order to secure the spin coated wafer on top of the substrate holder (Figure 11).

Once in the reactor chamber, the substrate holder was placed on top of an aluminum "bridge" which was situated in the middle of the reactor chamber. The bridge was held in place by four long screws. It is important that the "bridge" be held firmly in place. If it were not then the angle of the substrate to the oncoming stream of activated gas species might vary from experiment to experiment. This would alter the number of gas species impinging on the substrate per unit area. Laser interferometry measurements would also change from experiment to experiment if the "bridge" was not held in place. All experiments on the spin coated Si wafers and PE film were performed 22.2 cm (x+y+z in Figure 9) downstream from the plasma and all of the experiments on Kapton films were performed 21.8 cm downstream of the plasma. The 0.4 cm difference is due to the thickness of the compression fitting (Figure 10a).

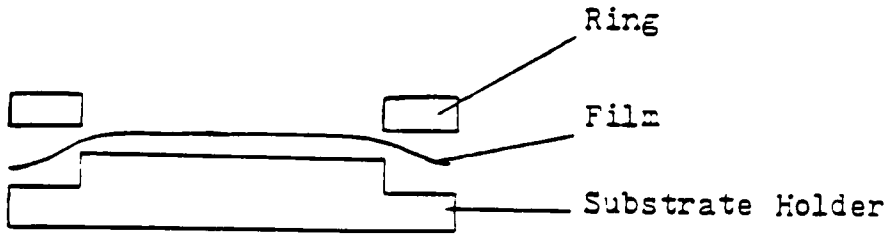

Figure 10a

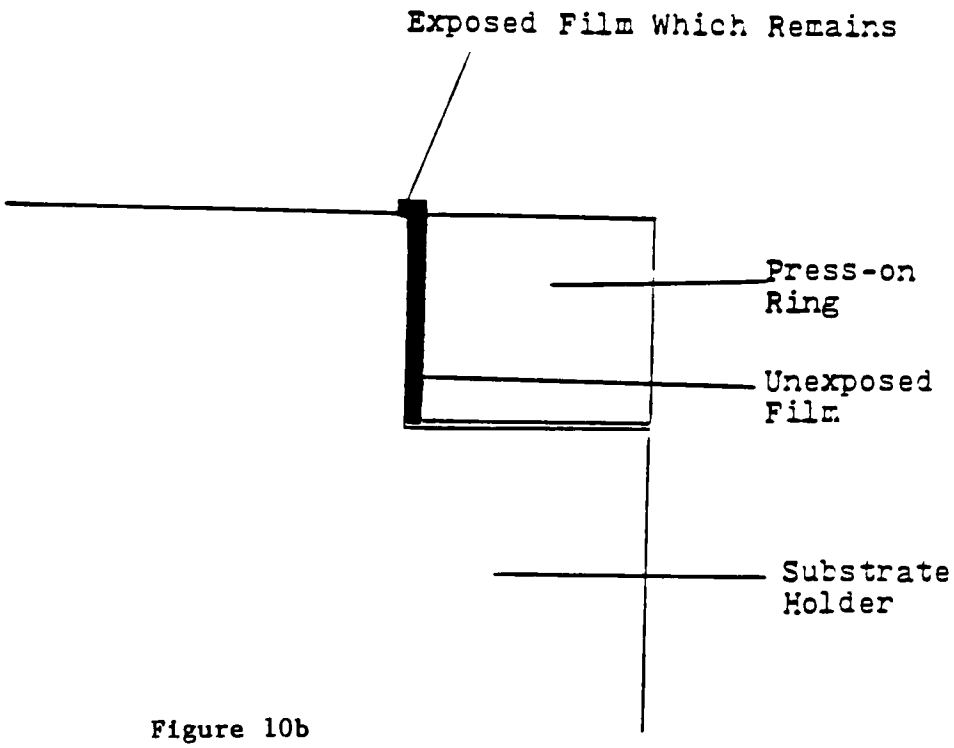

Figure 10b

Figure 10a. Sample holder for Kapton H film.
10b. Expanded view of Kapton H film held in place by ring.

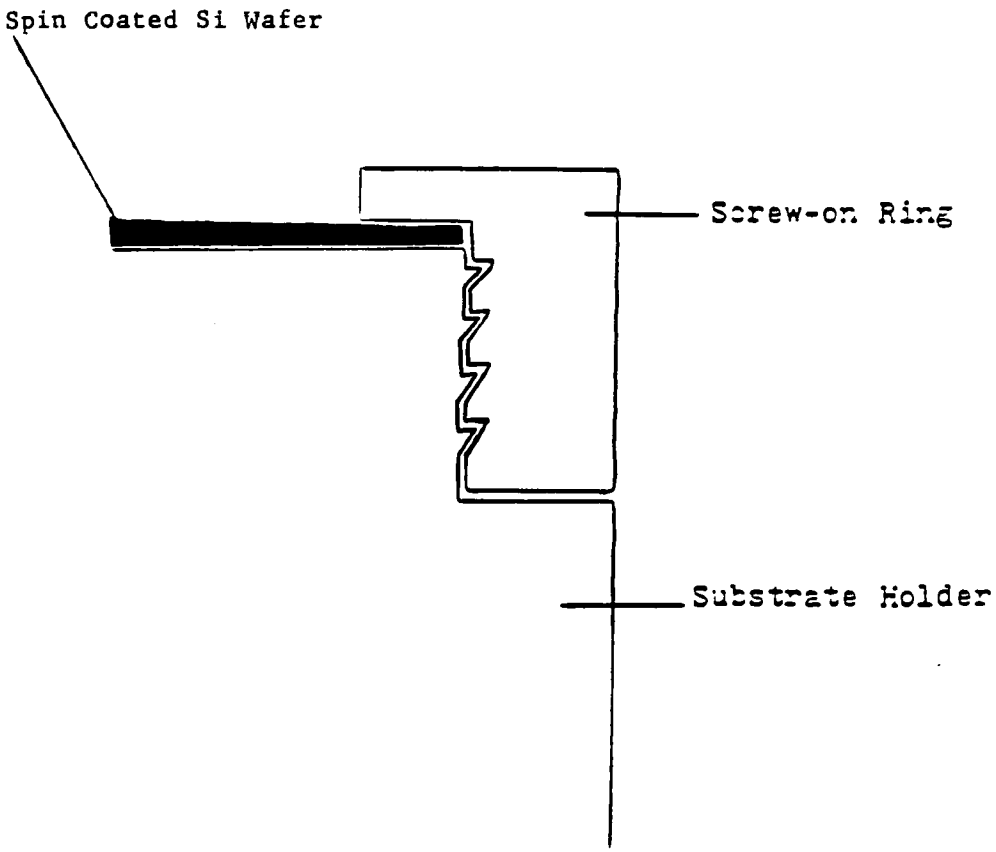

Figure 11. Sample holder for spin coated Si wafers.

2.1.2 Laser, Photodiode, Ammeter and Chart recorder

The four components listed above were used in order to determine etch rates and sample thicknesses. Etch rates were measured using laser interferometry. [23] Interferometry is a general term that refers to measurements of changing intensity due to constructive and destructive interference patterns (Figure 12). If the path difference between λ_1 and λ_2 is an integral number of wavelengths, then the waves interfere constructively. The laser beam reflects with maximum intensity. If the path difference is an odd number of half wavelengths, then the waves interfere destructively and the laser beam reflects with minimum intensity.

The equation:

$$d = \lambda / 2n \qquad (3)$$

gives the film thickness, d, between 2 successive maxima or 2 successive minima. λ is the wavelength of the laser beam and n is the index of refraction of the polymer. d is fixed because λ and n are constants.

The equation for etch rate is given by:

$$ER = v \times d / dpp \qquad (4)$$

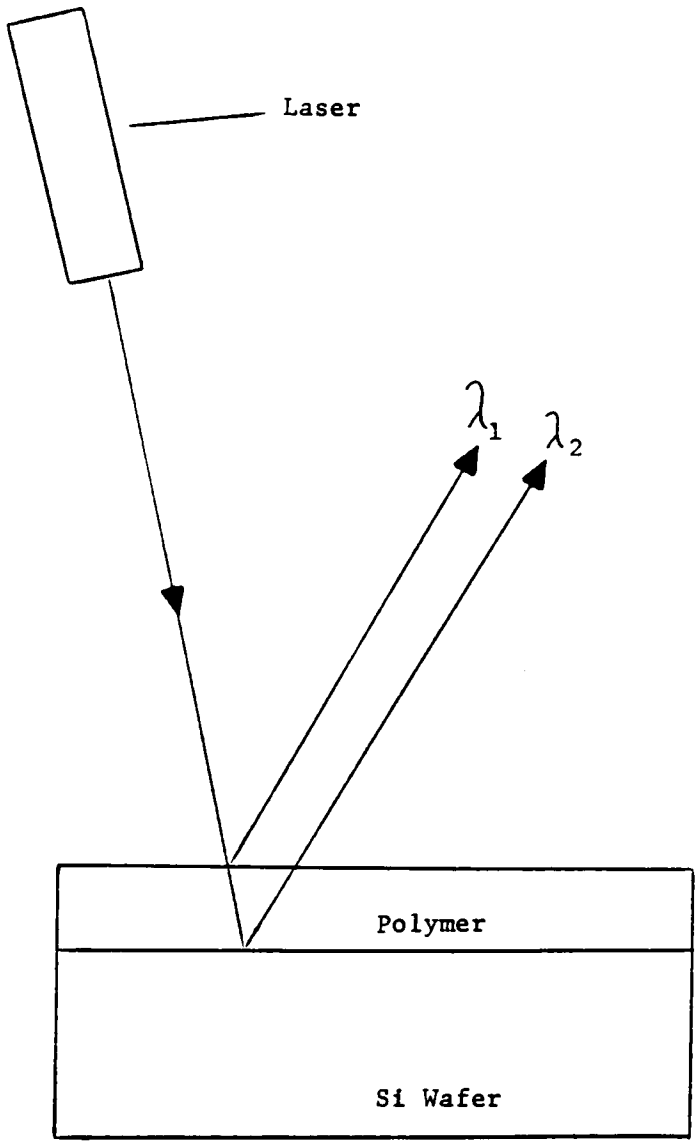

Figure 12. Schematic showing the technique of laser interferometry.

where v is the speed of the chart paper and dpp is the distance between peaks on the chart paper.

The thickness, t, of a sample that is etched, is the product of the film thickness, d, between 2 successive peaks (determined by equation 3) and the total number of peaks, which is taken directly off the chart paper. The equation is given by:

$$t = d \times (\#\ \text{of peaks}) \qquad (5)$$

A helium-neon laser beam (5 mW) with a wavelength of 632.8 nm was directed at near normal incidence onto the substrate. The beam went down the length of the quartz injector tube after passing through a polished Pyrex window. The window is located at the top of the quartz injector tube. A vacuum tight seal was achieved by using a 1" Cajon fitting. The male portion of the fitting was attached to the top of the quartz injector tube. The Pyrex window was placed inside the female portion of the fitting. Two Viton O-rings were needed, one on either side of the window, in order for a vacuum seal to be achieved when the male and female portion were brought together.

The reflected laser beam from the substrate was detected by a Spectra Physics Photodiode, Model # 404. The photodiode was connected to a Spectra Physic 404 power meter (ammeter). The ammeter can be varied in sensitivity from 0.02 mW to 5.0 mW depending on the intensity of the reflected laser beam.

One factor which affects reflected laser beam intensity is substrate thickness. When thicker samples were used, the reflected beam intensity decreased. Also, during the course of some experiments which involved etching, the reflected beam intensity decreased with time. The observed decrease in intensity with etching is due to surface roughing of the substrate. The rougher the surface became the less the laser beam specularly reflected; this lead to a decrease in detected laser beam intensity.

2.1.3 Pressure Gauges

A type 310 BHS-1 Torr absolute capacitance manometer pressure sensor was used to measure the reactor chamber pressure. The reactor pressure during experiments was 0.3 torr. For a visual display of the pressure, the sensor was connected to an MKS Baratron Type 170-M-270 digital readout unit.

A diaphragm in the pressure sensor deflects towards electrodes when the reactor chamber is being evacuated. This deflection causes a change in the capacitance between the diaphragm and each adjacent electrode on the reference side. Sensor electronics amplifies the signal that is produced by the change in capacitance between the electrodes and the diaphragm. In order to help minimize the effects that ambient temperature might have on the sensor zero, the

sensor is kept at a constant 45 C. Internal heaters which were controlled by a DC proportional control make this possible. [32]

A VCR to Swagelok connector was used to mate the capacitance manometer to a 1/4" stainless steel flexible tube. The tube in turn was connected to the reactor chamber using a 1/4" stainless steel ultra-torr male connector. One end of the fitting was threaded into the right-hand side aluminum plate. The threads were wrapped with teflon tape and a Viton O-ring was used in order to achieve a vacuum tight seal between the aluminum plate and the ultra-torr fitting.

In order to measure the pressure in the range from $5x10^{-3}$ torr to $1x10^{-9}$ torr, a NRC 524-2 cold cathode ionization gauge was used. The gauge was connected to a NRC 855 vacuum ionization gauge controller. The gauge was attached to the vacuum system by using an O-ring compression adaptor.

2.1.4 Gas Flow Readout Unit and Mass Flow Controllers

The gases used in the experiments were O2, CF4 and Ar. The gas composition for etching and removal of passivation experiments varied depending on the polymer which was being studied. The gas composition for all passivation experiments was: 85% CF4, 10% O2 and 5% Ar. These percentages were

chosen because they generated the greatest number of F atoms in the plasma according to spectral line intensity measurements (Figure 13). The total flow rate was 52 sccm for all experiments.

Gas flow rate was controlled by Tylan FC-260 mass flow controllers. Mass flow control is a means of measuring and automatically controlling the weight flow rate of a gas. A sensor tube externally wound with 2 heated resistance thermometers is used to measure the gas flow. A bridge circuit senses the temperature differential and develops a linear output signal of 0 to 5 Vdc proportional to the gas flow rate over the calibrated range. The output signal is then compared to a command voltage from a voltage source. This comparison generates an error signal that alters the valve power, thereby changing the flow rate until the set point is reached. [33] During the experiments, the mass flow controllers were controlled and monitored by a Tylan RO-14 readout unit.

The 3 mass flow controllers (one for each gas) were connected to 1/4" stainless steel tubing. The tubing in turn was connected to 1/4" flexible stainless steel tubing which was connected to the quartz injector tube. A 1/4" stainless steel Cajon ultra-torr male connector provided a vacuum tight seal between the injector tube and the flexible tubing.

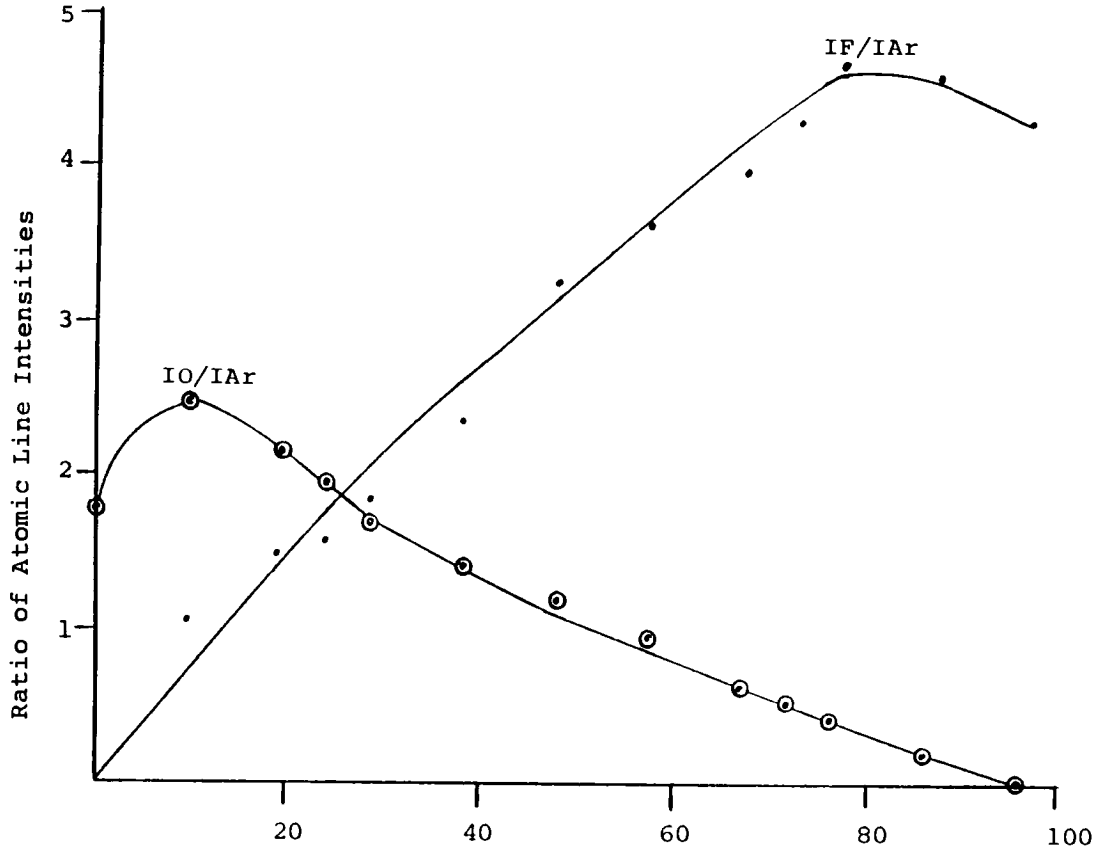

Figure 13. Ratio of the atomic line intensities OI 845/ArI 750 nm and FI 704/ArI 750 nm as a function of CF_4 concentration in an O_2-CF_4-Ar microwave plasma.

2.1.5 Microwave Source and Microwave Clip-on Cavity

A Micro-Now Instrument, Model 420B, 2.45 GHz power source supplied the MW power to an Opthos Instruments "Everson" type air-cooled clip-on cavity. The cavity was clipped on to the quartz injector tube. The power supply, which has an output power rating from 0 to 500 watts, was connected to the clip-on cavity by means of a coaxial cable. By inductively tuning the clip-on cavity, the reflected power for all experiments was nearly equal (< 2 watts) to zero watts.

The center of the cavity to the center of the injector tube was 5.3 cm (x-distance in Figure 9) for all experiments. The difference between the forward and reflected power was taken to be the absorbed power. The absorbed MW power for all experiments was between 58-60 watts. In order to ensure that the MW power was stable throughout the course of an experiment, the power source was connected to a Sola constant voltage normal-harmonic type transformer.

2.1.6 Vacuum System

The vacuum system consisted of a water-cooled, 6" oil diffusion pump, backed by a Balzers Type DUO 35 mechanical pump. Tyreno 12 pump oil, which is a fluorocarbon oil, was used in the mechanical pump. Since O atoms can react violently with a hydrocarbon oil, Tyreno 12 pump oil was used in order to eliminate the chance of an explosion within the mechanical pump.

An IBM Central Scientific Auto-Manual Vacuum Control System was used to control the valves (high vacuum, foreline and roughing) as well as the diffusion pump. A Model 100L Cyrotrol controller was used to control the liquid nitrogen fill into the diffusion pump trap.

The vacuum system was connected to the bottom aluminum plate of the reactor chamber via a 2" (5.08 cm) i.d. copper tubing and elbows. To vary the pressure inside the reactor chamber a type SL inline Viton O-ring sealed brass Veeco valve was installed using silver solder connection in the middle of the copper tubing. All of the connecting plumbing and throttle valve was leak tested with a helium leak detector.

2.2 Substrate Analysis

2.2.1 Gravimetric Analysis

Gravimetric analysis of the spin coated polyimide samples was done using a Mettler Type M5 microbalance. The samples were weighed before and after exposure to the fluorine-rich plasma. The microbalance has a sensitivity of $1x10^{-5}$ grams.

The "corresponding thickness" equation converts a weight loss into a thickness loss. The equation is given by:

$$h = (w/\pi r^2)/\delta \qquad (6)$$

where h is the "corresponding thickness" of the etched material beneath the fluorinated layer, w is the weight loss due to the etching of the top fluorinated layer and the unmodified polyimide beneath the fluorinated layer, r is the radius of the sample and δ is the density of PI. A density of 1.43 g/cm^3 [34,35] was used in the calculations.

2.2.2 X-ray Photoelectron Spectroscopy

X-ray photoelectron spectroscopy (XPS) analysis was performed at IBM, Endicott. The instrument was a 560 Physics Electronics AES/XPS spectrometer. The change in atomic percent at the surface during the passivation, removal of passivation, and etching was studied.

2.2.3 Scanning Electron Microscopy

An ISI-40 International Scientific Instrument scanning electron microscope was used to analyze the surface morphology of various polymer samples which had been: 1) passivated then etched, 2) passivated without etching and 3) etched without passivation. Photomicrographs of the samples were taken using Polaroid Type 53 film. Magnification of the photomicrographs varied from 0.52kx to 6.0kx. The filament voltage was kept constant at 15 kV. Before the polymer samples were placed into the SEM, an Au/Pd film was sputtered onto the samples.

By use of double-stick tape, the samples were centered and fixed onto an SEM sample stud. This method was used when viewing the top side of a sample. To obtain an edge-on view of a spin coated polyimide sample, the wafer scribed on the backside (side without spin coated polyimide) and then was

broken in half. The polyimide was then cut with a razor blade. In order to reduce the effect of smearing of the polyimide sample caused by the cutting with the razor, the sample half was placed in the reactor chamber and was exposed downstream of an oxygen-rich plasma for four minutes. Afterwards, the sample half was fixed vertically onto a sample stud (Figures 14a and 14b).

The sputtering process was performed in a Polaron Instruments Inc. SEM coating unit E 5000. After the sputtering process was completed, Ar was allowed to flow into the chamber for a period of 2 to 3 minutes. This was done to ensure that the newly sputtered coating would not be oxidized. An oxidized coating will decrease the resolution of a photomicrograph.

2.2.4 Goniometry

An NRL Contact Angle Goniometer Model 100-00 was used for the contact angle measurements. Two microliters of distilled water was used for all contact angle measurements.

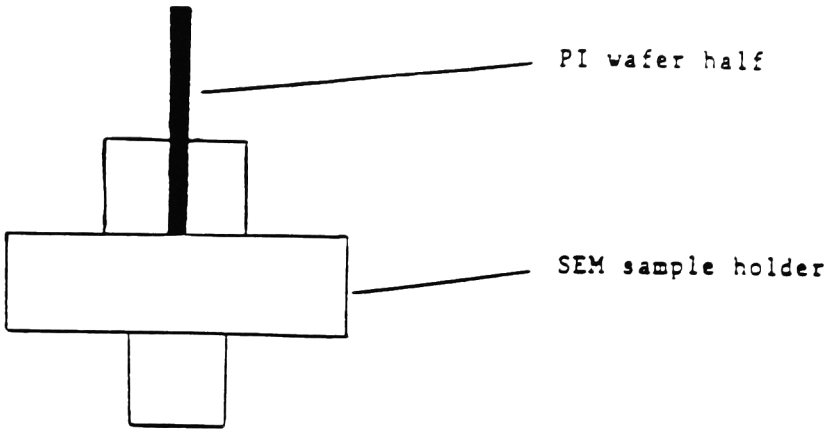

Fig 14a Front view of vertically fixed PI wafer.

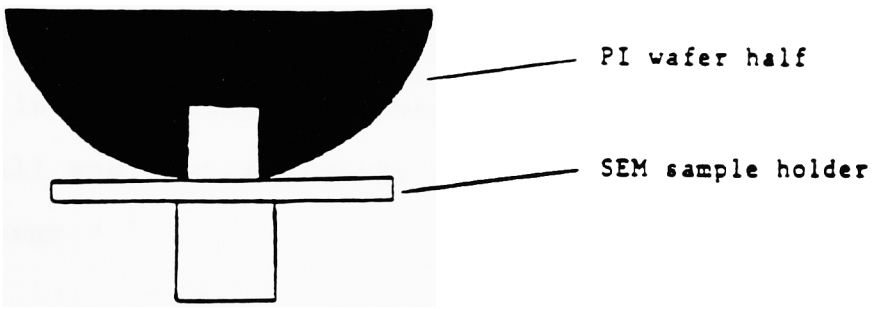

Fig 14b Side view of vertically fixed PI wafer.

Contact angle, θ, measurement is a commonly used technique for analyzing the wettability of a surface. A surface is considered wettable (low surface energy) if $\theta < 90$ and non-wettable (high surface energy) if $\theta > 90$. One characteristic of highly fluorinated surfaces is that they are non-wettable. [36]

θ is defined by Young's Equation:

$$\theta = \cos^{-1} ((\gamma_{SV} - \gamma_{SL}) / \gamma_{LV}) \qquad (5)$$

where γ is the interfacial tension, measured in mJ/m^2, at each of the three interfaces: solid, S,; liquid, L, and vapor, V (Figure 15). [37]

It is not an easy task to extract the exact value of the surface energy via a contact angle measurement. Fortes [37] has described in detail the complexities associated with evaluating contact angle measurements and the theory of wettability.

A very general approach will be made when interpreting the contact angle measurements. That is, a high contact angle will indicate that a polymer has a low surface energy while a small angle will signify that a polymer has a higher surface energy.

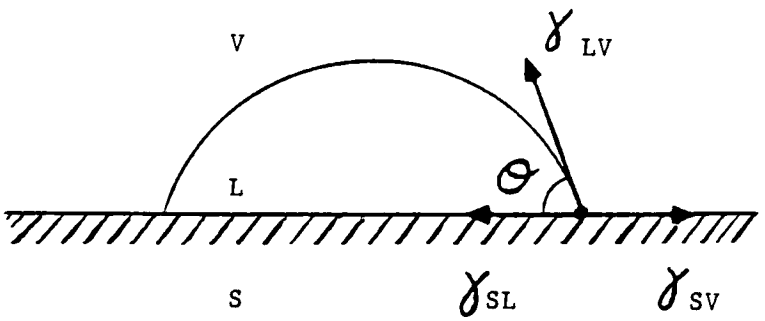

Figure 15. Contact angle, θ, formed at a polymer surface. V represents vapor (usually air), S-polymer surface, L-liquid (usually water) and γ is the interfacial tension.

2.3 Sample Preparation

2.3.1 Polyimide

Two ml of polyamic acid (obtained from IBM, Endicott) was applied to 57.15 mm diameter silicon wafers using a Brinkman Dispensette. The wafers were then placed in a Headway Research Model 1-EC101D-R485 photoresist spinner. The spinning speed and duration of spin was controlled by a Headway Research Spin Controller unit. The wafers were spun at 3000 rpm for 5 seconds. At the end of the spin cycle, automatic dynamic braking stopped the spinner quickly.

After the wafer was evenly coated it was placed on an 8 1/4" by 3 1/2" three-tiered wafer rack (4 wafers per tier). The full rack was placed in a Thermolyne Model F-D 1525M Furnace. The substrates were initially heated at 85 C for 15 minutes in air. After the 15 minutes, nitrogen was allowed to flow into the furnace. The temperature was then automatically ramped from 85° C to 360° C over a 2 hour period. Once at 360° C, the temperature was kept constant for an additional 30 minutes; after which the wafers were removed from the oven and allowed to cool. The automatic ramping was accomplished by using an Omega Series CN-2010 programmable temperature controller.

2.3.2 Polyvinyl Alcohol

Six grams of polyvinyl alcohol (obtained from Aldrich Chemical Co.), in granular form, (99.7% Mole Hydrolyzed, M.W. 108,000 g/mol) was dissolved in 500 ml of a 50-50 ethanol-water solution. The solution was heated and magnetically stirred until 400 ml of the solution was evaporated. The remaining 100 ml of the solution was viscous and clear.

Four ml of the solution was pipetted onto an Si wafer. The substrate was spun at 1500 rpm for 5 seconds. The samples were cured in an oven under atmospheric conditions at 50°C for a period of 2 hours.

2.3.3 Polybutadiene

Sixty grams of polybutadiene (obtained from Aldrich Chemical Co.), in slab/chunk form, (M.W.200,000 g/mol to 300,000 g/mol) was placed in 1000 ml of tetrahydrofuran. The mixture was heated and magnetically stirred until 750 ml remained. The remaining solution was viscous and clear.

Four ml of the solution was pipetted onto an Si wafer. The substrate was spun at 2000 rpm for 10 seconds. The wafers were then cured in a vacuum (30 mm Hg) oven for 48 hours at 70°C.

Polybutadiene was used in the etching experiments, but not in the contact angle measurement experiments. The main problem encountered in the preparation of the polybutadiene solution was obtaining a solution that was viscous enough to be spin coated onto an Si wafer.

2.3.4 Polystyrene

Thirty grams of polystyrene (obtained from Aldrich Chemical Co.), in pellet form, (M.W. 250,000 g/mol) was placed in 500 ml of THF. The mixture was heated and automatically stirred until 100 ml remained. 4 ml of the viscous, clear solution was spun onto an Si wafer at 2000 rpm for 5 seconds. The substrates were cured in a vacuum (30 mm Hg) oven for 20 hours at 70° C.

2.3.5 Polyethylene

Polyethylene (low density) was obtained in sheet form from Quality Packing Supply Corp., Rochester, NY. By use of a heat gun, the Si wafer was heated to approximately 200° C. A circular, pre-cut piece of the PE film was placed on top

of the hot Si wafer and was rolled down using a glass tube in order to adhere the film onto the Si wafer.

2.3.6 Kapton H (a brandname of PI)

Kapton H was obtained from DuPont. The thickness of the film was 40 micrometers.

3.0 RESULTS

3.1 Etch Rate for Structurally Different Polymers vs. % O2 in the Gas Feed.

In this study, the following five polymers were used: polystyrene (PS), polyvinylalcohol (PVA), spin coated polyimide (PI), polyethylene (PE) and polybutadiene (PB) (Table 2). These polymers were selected because of their structures. PS and PI are aromatic, PVA and PE are saturated and PB is unsaturated.

The polymers were exposed downstream of the MW plasma. The percentage of O2 in the gas feed varied for each experiment. The etch rates of the polymers were obtained from laser interferometry. The results of the experiments are shown in Figure 16.

Table 2

Structure of Polymers

Polystyrene	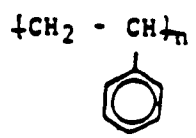
Polybutadiene	
Polyvinylalcohol	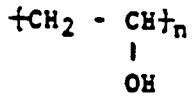
Polyethylene	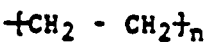
Polyimide	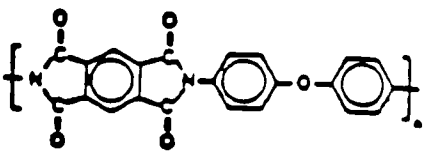

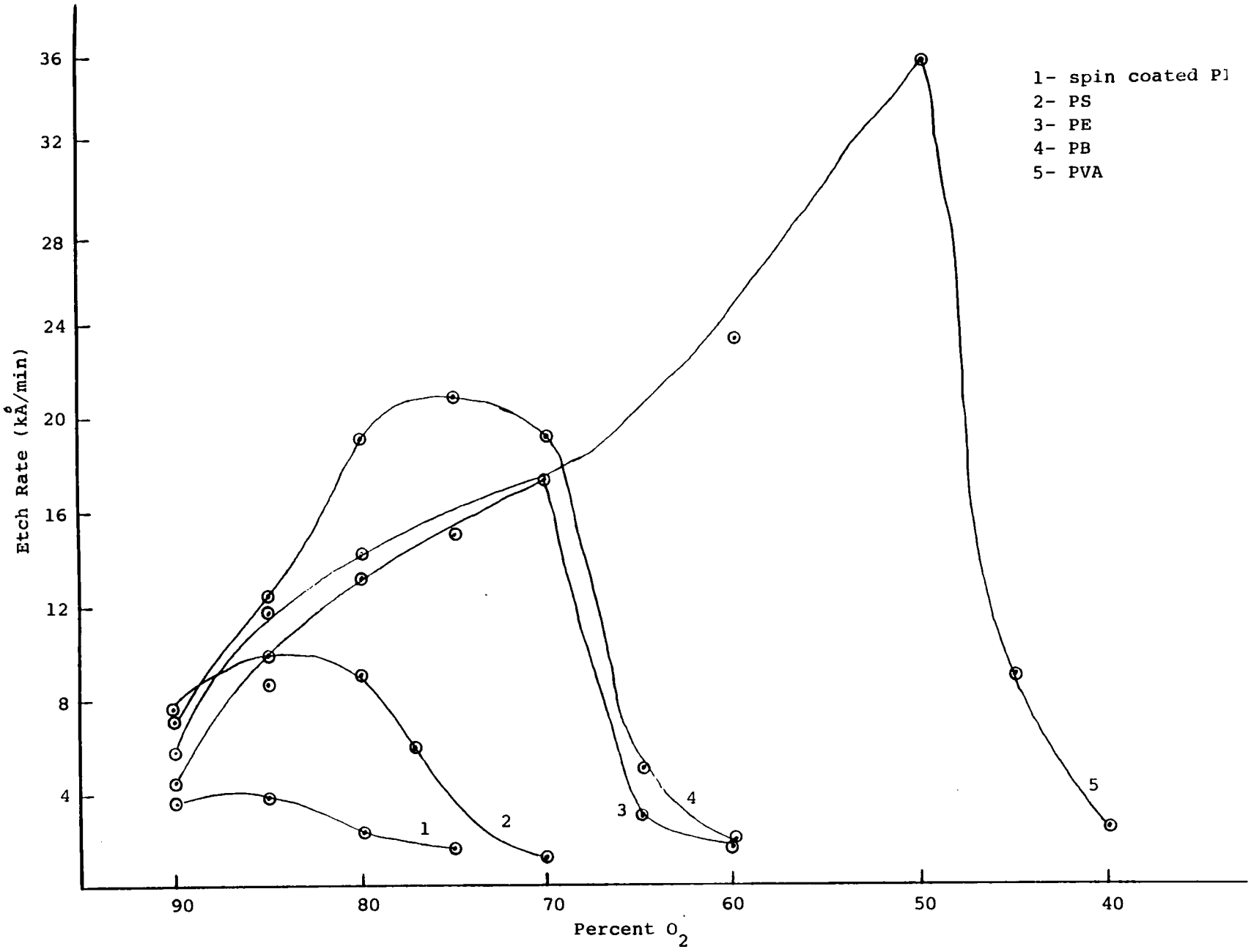

Figure 16. Etch rate vs. percent O_2 for Structurally Different Polymers Downstream of an O_2-CF_4-Ar Microwave Plasma.

3.2 Contact Angle Measurement Experiments

A series of experiments were carried out in order to establish what the effect of varying the gas composition would have on the contact angles of the exposed polymers. The polymers used were: PVA, PS, PE and Kapton H. PB was not used becaused of the difficulties (Refer to 2.3.3) that arose during its preparation. Spin coated PI was also not used.

The exposure time downstream of the MW plasma was one minute. The percentage of O2 in the gas feed varied for each experiment (Table 3). Contact angles were taken directly after the one minute exposure period by using a NRL C.A. Goniometer, Model # 100-00 115. The volume of the drops was 2 microliters. Three drops yielded 6 contact angle measurements per wafer. The average of the 6 readings along with the standard deviation is given in Table 3. Figure 17 is the graph of Table 3. In a few experiments, the interface between the water drop and the substrate was not sharp. As a result, the contact angles were estimated to be less than 5 degrees.

Table 4 shows the contact angles of the polymers before they were exposed to the plasma; the table also gives the maximum contact angle that the polymer achieved and the percent difference between the two.

Table 3

Results of contact angle measurements for experiments performed downstream of a CF4-O2 mixture containing 5% Ar.

% O2	Polymer	Ave. Cont. Angle (deg)	Std. Dev. (deg)
90	PE	67	2.3
80		61	1.8
70		52	1.6
60		19	2.2
50		5	0.71
40		73	0.9
30		95	10.6
20		128	4.4
15		136	2.5
10		134	4.3
0		120	1.3
85	Kapton H	10	--
75		13	0.71
65		12	0.71
60		12	0.71
50		13	0.71
40		12	1.3
30		15	1.4
20		78	7.9
15		97	0.41
10		98	0.42
0		90	0.89
95	PVA	19	3.4
90		23	0.89
80		<5	--
70		<5	--
65		14	1.6
50		31	1.7
40		60	2.2
20		89	0.95
15		111	1.3
10		109	2.7
0		92	1.5
80	PS	16	1.9
70		<5	--
60		<5	--
50		<5	--
40		<5	--
20		108	0
15		110	1.6
10		115	1.5
0		100	1.6

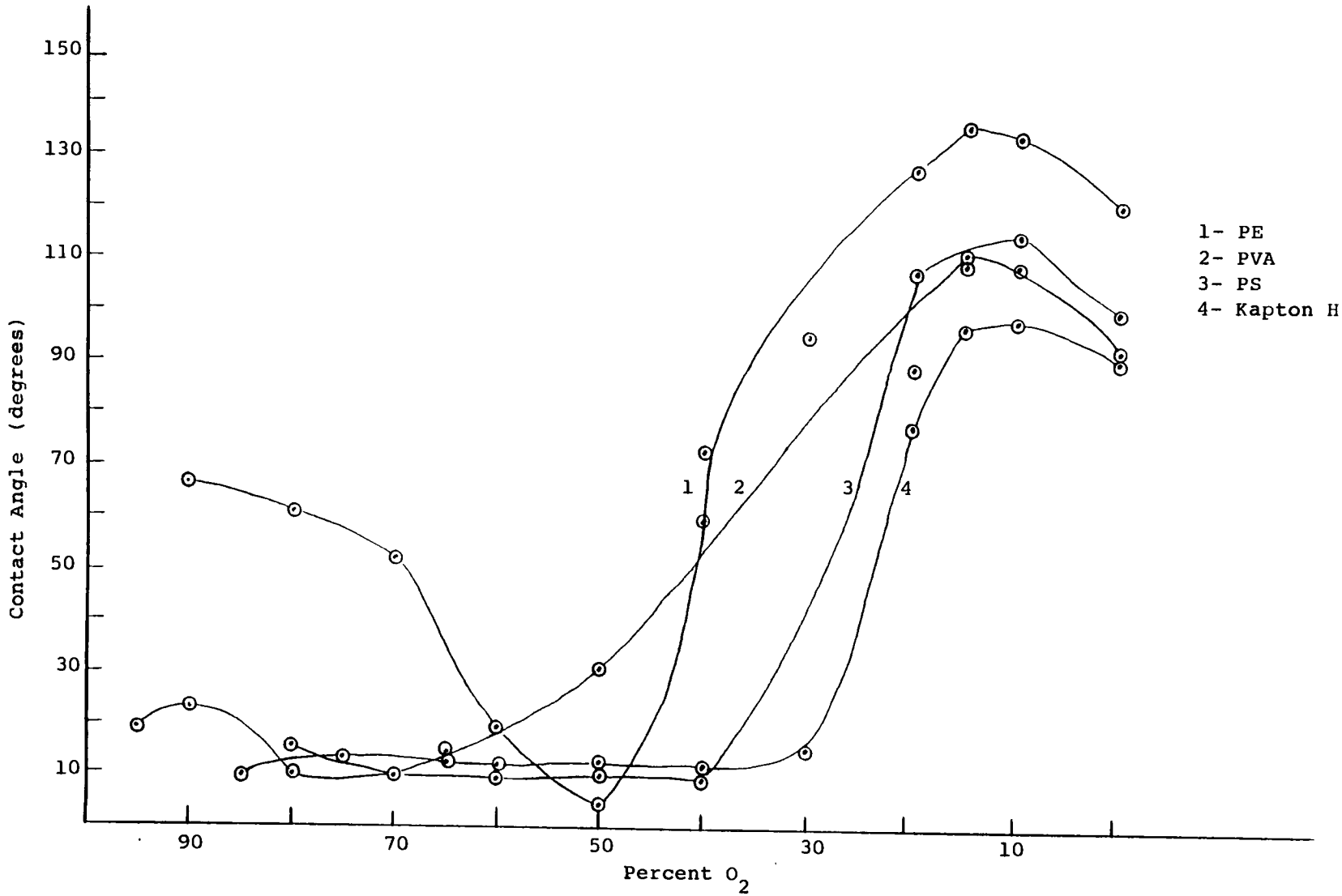

Figure 17. Variatons in Contact Angles for Structurally Different Polymers Exposed Downstream of an O_2-CF_4-Ar Microwave Plasma.

Table 4

Comparison of contact angle measurements, of various polymers, taken before exposure to the CF4-O2-Ar MW plasma and the maximum values obtained after exposure to the MW plasma.

Polymer	Angle Before Plasma (deg)	Maximum Angle (deg)	% Difference
Kapton H	78 ± 3.5	98 ± 0.42	20.2
PE	89 ± 0.8	136 ± 2.5	65.4
PVA	61 ± 1.9	111 ± 1.3	55.0
PS	91 ± 0.8	115 ± 1.5	20.9

3.3 Removal of Fluorination Experiments

Three spin coated PI samples (11 microns thick as determined by laser interferometry) were fluorinated for 20, 46 and 120 minutes. Each sample was then exposed to an O-rich plasma in order to remove the fluorinated layer. A nearly linear time dependency was observed for the time of fluorination and the time of removal of passivation (Figure 18). That is, for 20 minutes of passivation the time to remove the fluorinated layer (determined by the resumption of fast etching) was approximately 30 minutes. For 46 minutes of passivation, the time of removal was approximately 60 minutes and for 120 minutes of passivation, the time to remove the passivated layer was approximately 140 minutes.

Four spin coated PI samples were exposed downstream of a F-rich plasma for 20,30,46 and 60 minutes. The substrates were then exposed to an O-rich plasma. Figure 19 is the graph of weight loss of the fluorinated substrates vs. time of exposure to the O-rich plasma. Figure 20 is the etch rate of the fluorinated samples vs. time of exposure to the O-rich plasma. For samples previously fluorinated for 20,30,46 and 60 minutes, the "corresponding thickness" and total weight loss after 20 and 30 minutes of exposure to an O-rich plasma are given in Tables 5 and 6, respectively.

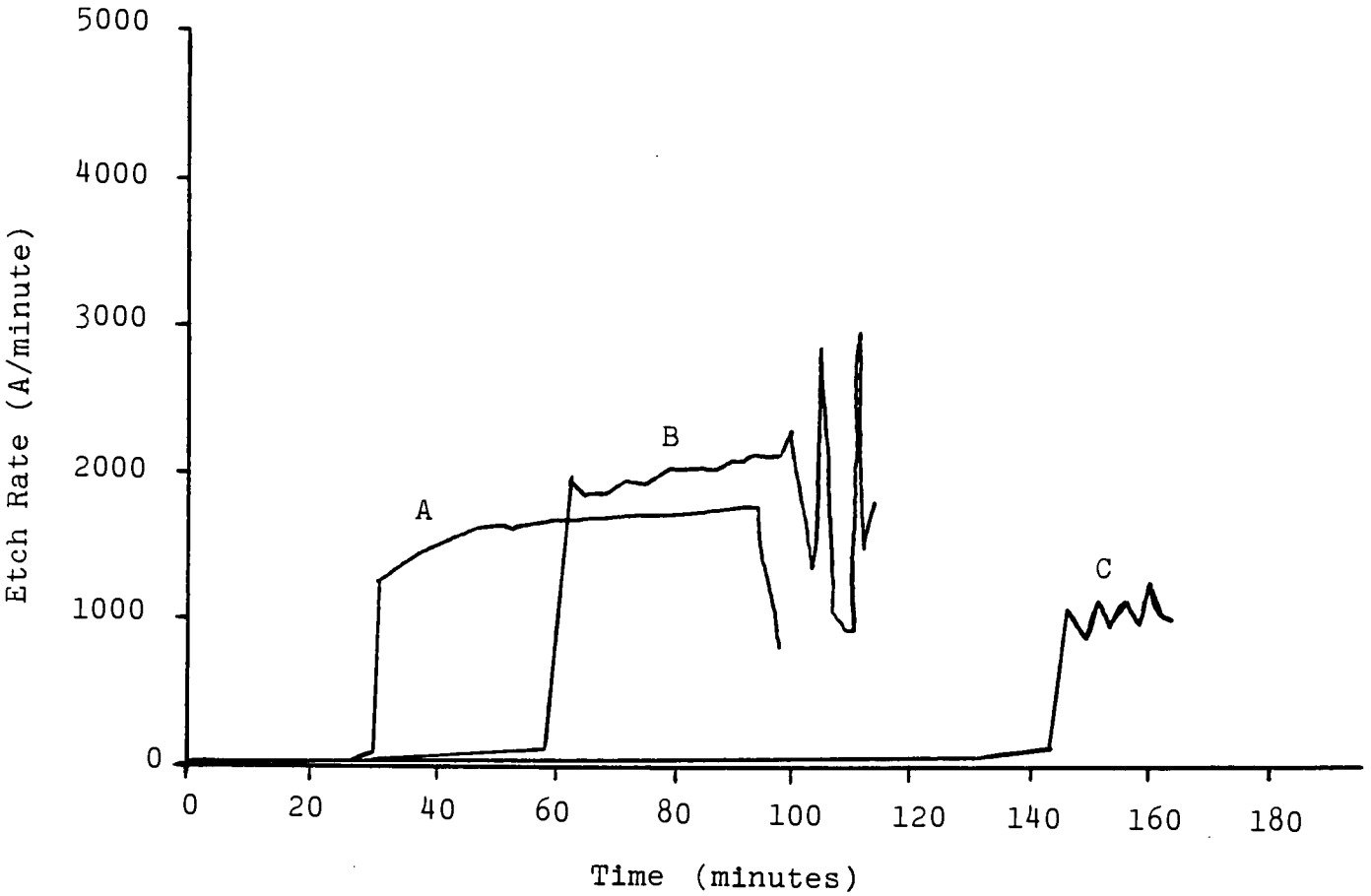

Figure 18. Etch rate, obtained by laser interferometry, as a function of time of exposure of the spin coated PI substrates to an oxygen-rich plasma. Previously the substrates were exposed to a fluorine-rich plasma for (A) 20 min., (B) 46 min. and (C) 120 min.

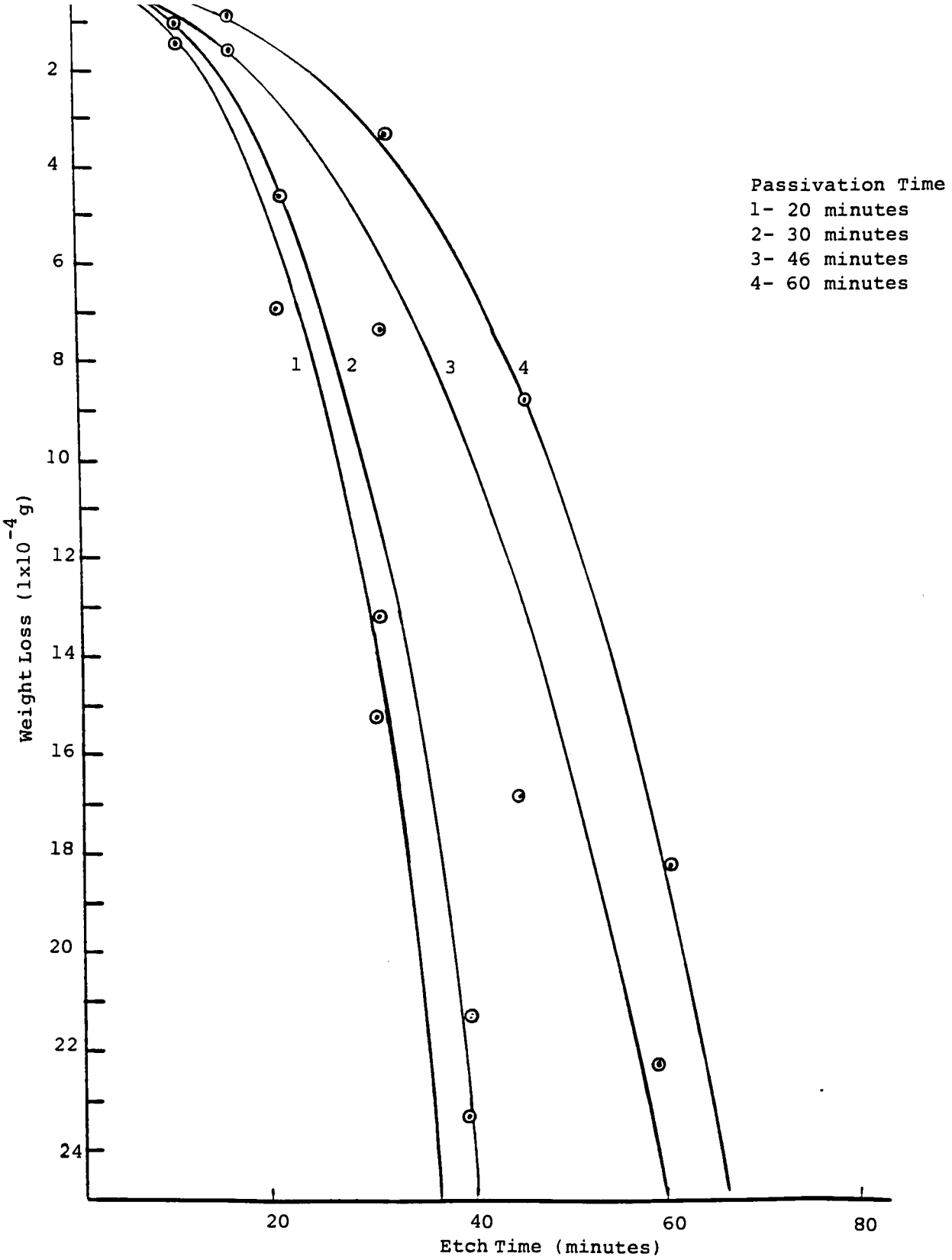

Figure 19. Weight Loss of Passivated PI Samples as a Function of Etch Time.

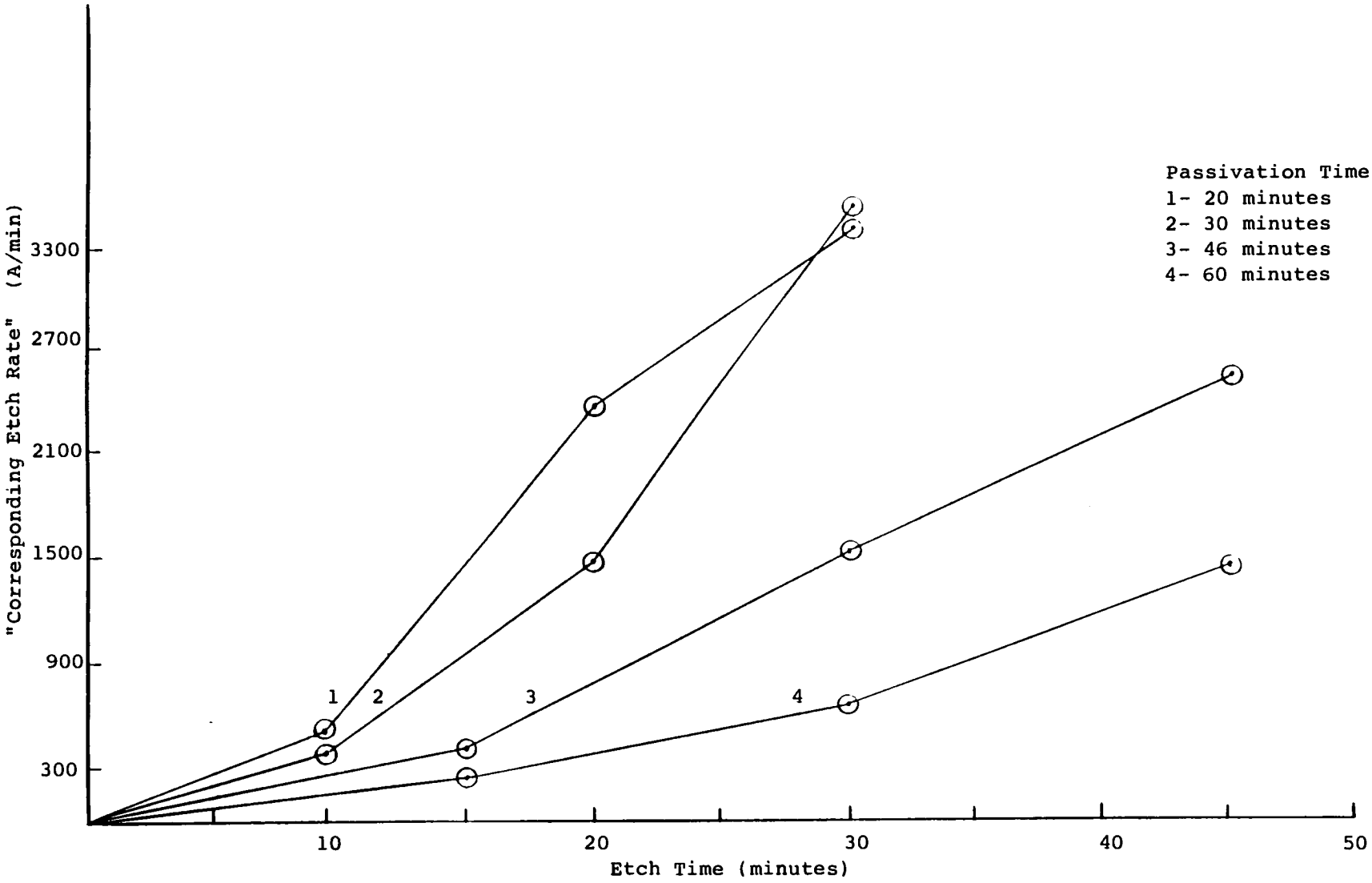

Figure 20. "Corresponding Etch Rate" of fluorinated PI spin coated wafers as a function of time of exposure downstream of an oxygen-rich plasma.

Table 5

Weight loss following 20 minutes of etching with an oxygen-rich plasma on previously fluorinated polyimide substrates.

Time of Previous Fluorination [min.]	Weight Loss [g]	"Corresponding Thickness" [A]
20	6.90×10^{-3}	29,239
30	4.65×10^{-3}	19,704
46	2.48×10^{-3}	10,509
60	1.42×10^{-3}	6,017

Table 6

Weight loss following 30 minutes of etching with an oxygen-rich plasma on previously fluorinated polyimide substrates.

Time of Previous Fluorination [min.]	Weight Loss [g]	"Corresponding Thickness" [A]
20	15.3×10^{-3}	64,833
30	13.2×10^{-3}	55,935
46	7.15×10^{-3}	30,298
60	3.20×10^{-3}	13,560

Table 7 shows the "corresponding thickness" and total weight loss for four PI samples. The first and second samples were fluorinated for 20 and 30 minutes, respectively, then were etched for 40 minutes. The third and fourth were fluorinated for 46 and 60 minutes, respectively, then were etched for 60 minutes.

3.4 Scanning Electron Microscope Investigations

A series of investigations were done using an International Scientific Instruments (ISI-40) scanning electron microscope (SEM). A total of 22 micrographs were taken of samples that were exposed to F-rich and O-rich plasmas for differing periods of time.

Figures 2 and 21-29 are of modified 40 micrometer thick Dupont Kapton H film. The micrographs of these figures were taken at the center of the surface of the samples.

Four spin coated PI samples were fluorinated for 30 minutes and then exposed to an O-rich plasma. Figures 22-25 shows the surface after 10,20,30 and 50 minutes of exposure to the O-rich plasma, respectively. The diameters of the holes, that formed during the removal of the passivated layer, are shown in Table 8.

In another series of experiments, the fluorination time varied from 30 to 60 minutes while the time of exposure to the O-rich plasma was held constant at 30 minutes. The

Table 7

Weight loss after 40 minutes of etching of polyimide substrates previously fluorinated for 20 and 30 minutes. Weight loss after 60 minutes of etching of polyimide substrates previously fluorinated for 46 and 60 minutes.

Time of Previous Fluorination [min.]	Weight Loss [g]	"Corresponding Thickness" [A]
20	23.3×10^{-3}	98,733
30	21.3×10^{-3}	90,258
46	22.2×10^{-3}	94,072
60	18.2×10^{-3}	77,122

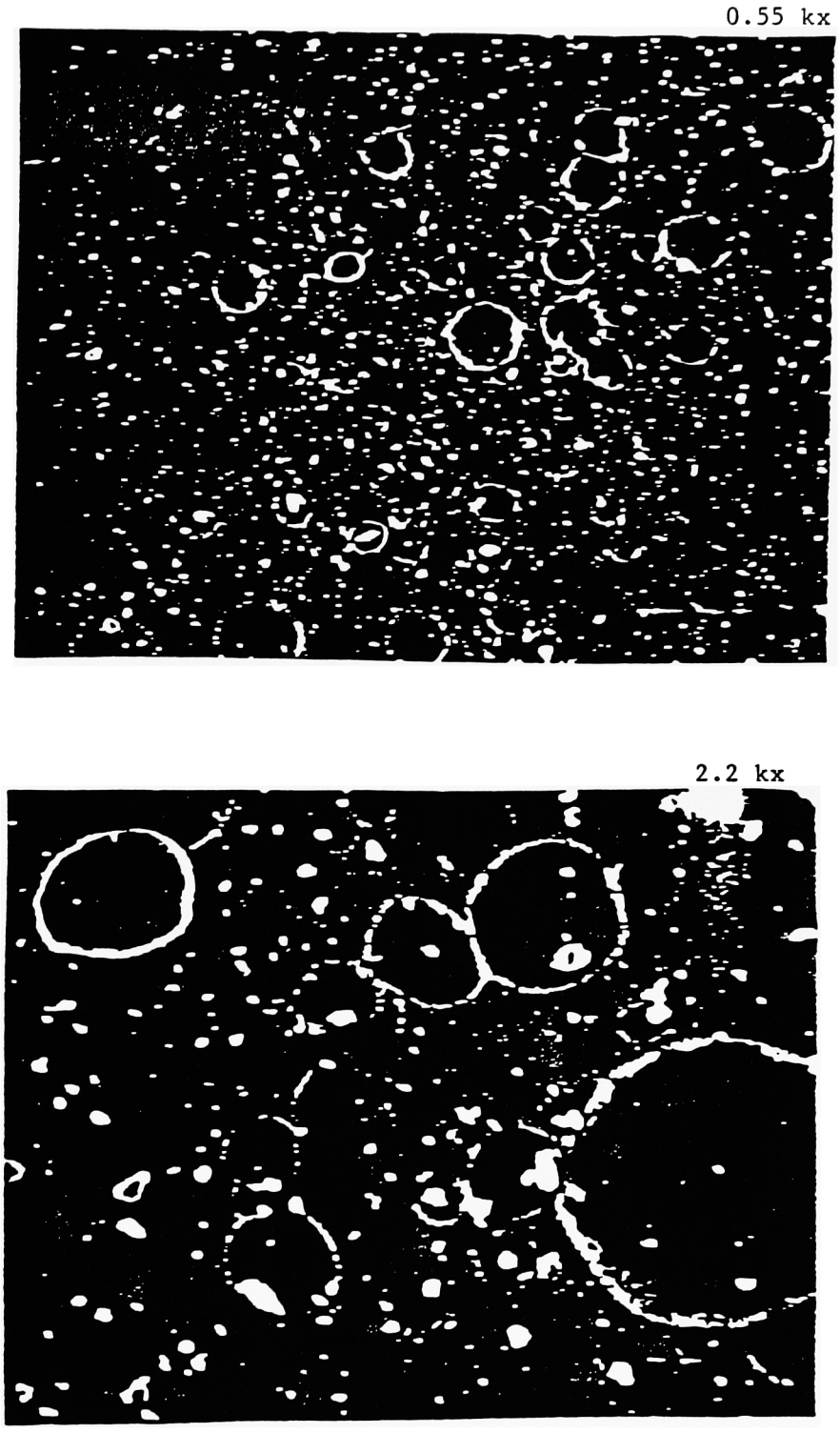

Figure 21. SEM micrographs of Kapton H that was etched for 70 minutes.

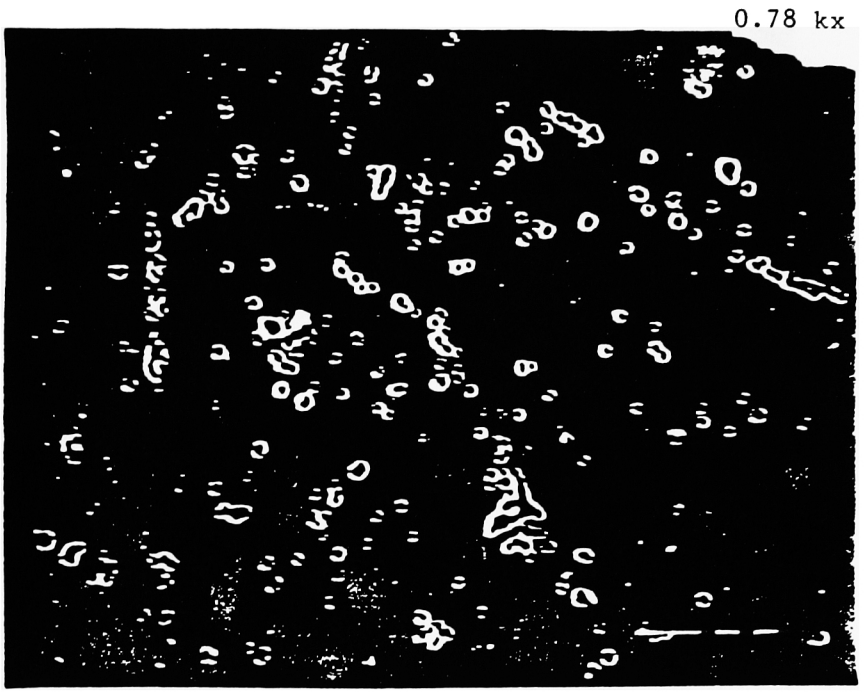

Figure 22. SEM micrograph of Kapton H that was fluorinated for 30 minutes and then etched for 10 minutes.

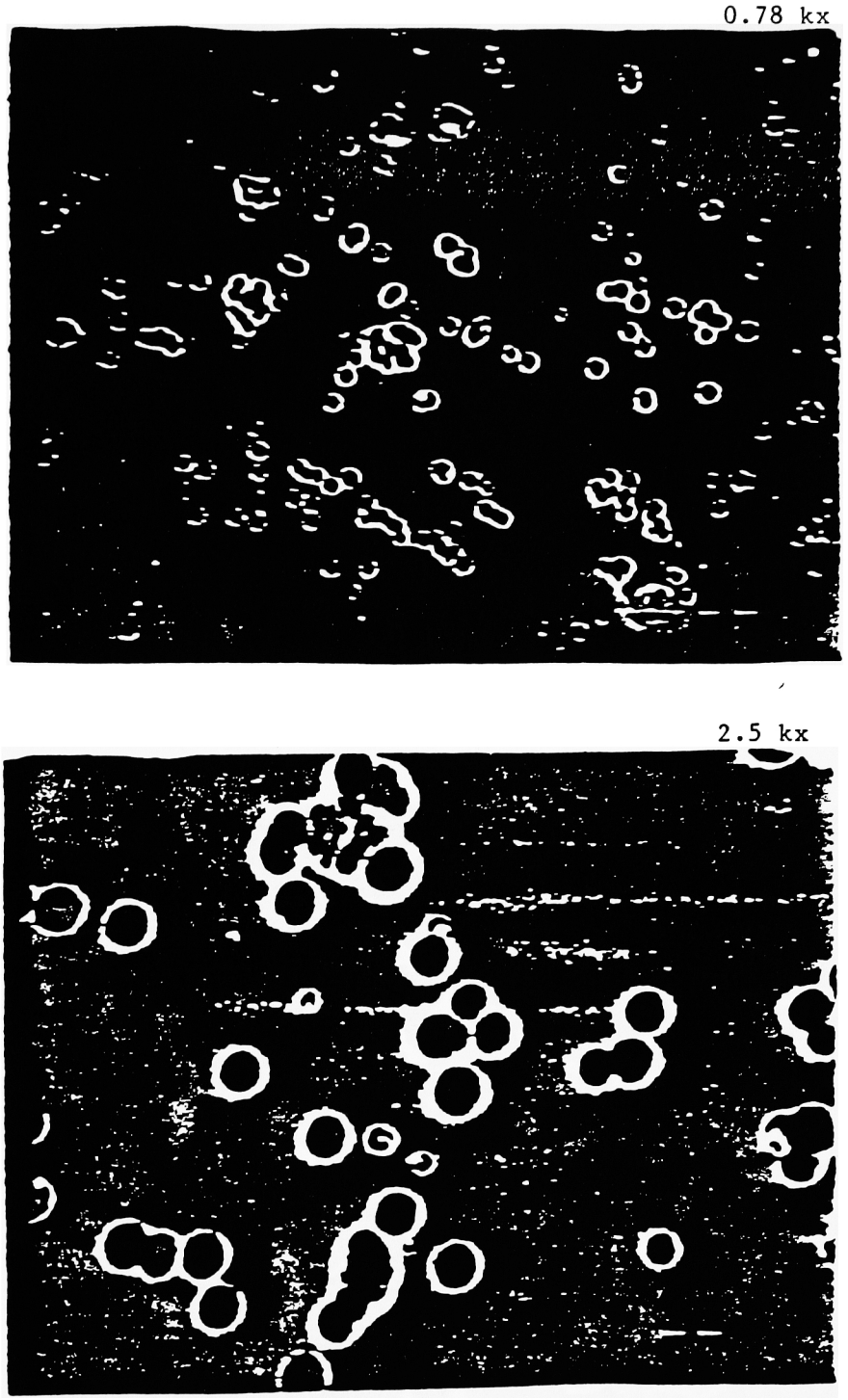

Figure 23. SEM micrographs of Kapton H that was fluorinated for 30 minutes and then etched for 20 minutes.

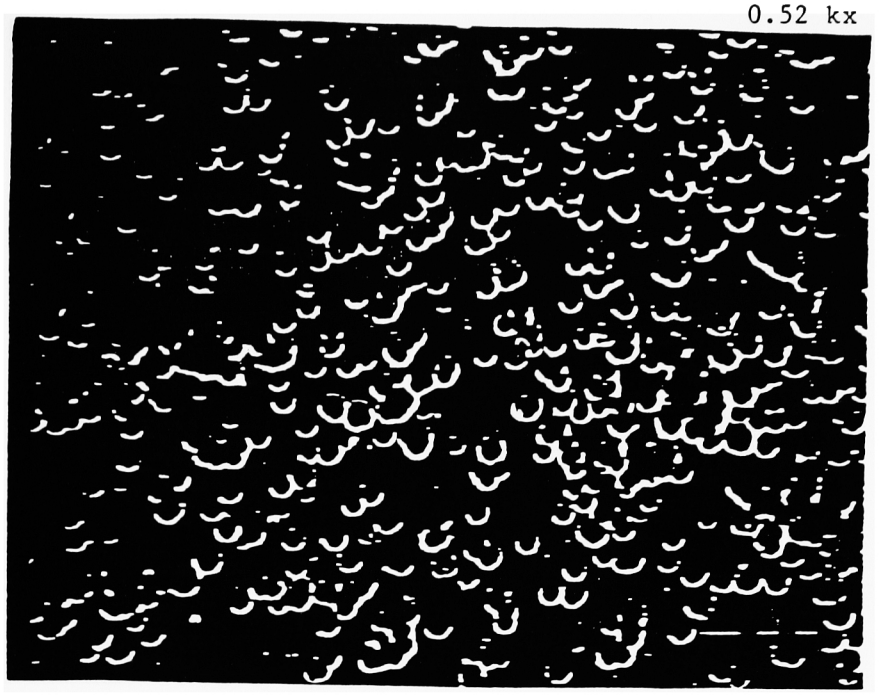

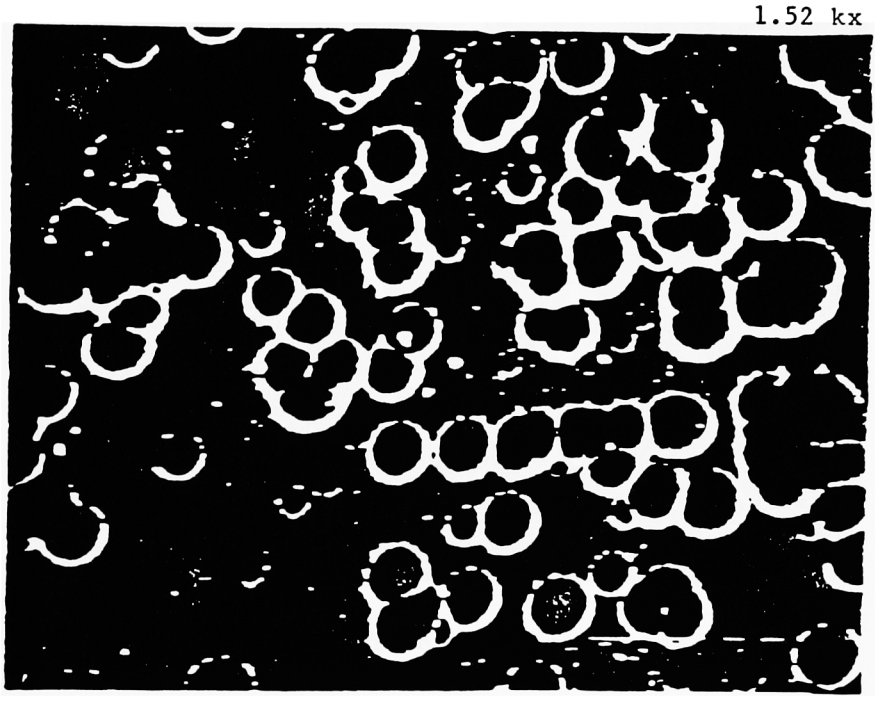

Figure 24. SEM micrographs of Kapton H that was fluorinated for 30 minutes and then etched for 30 minutes.

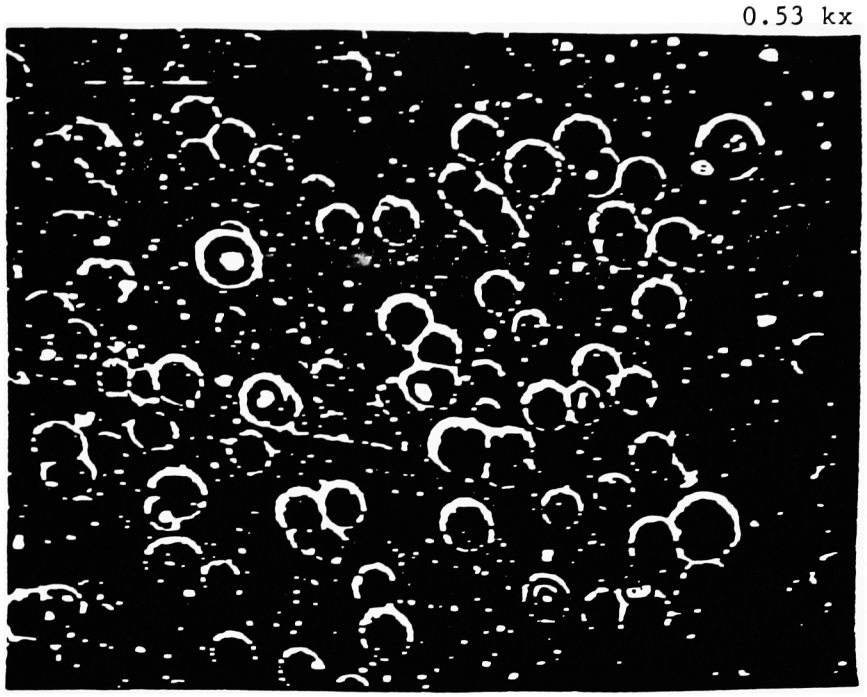

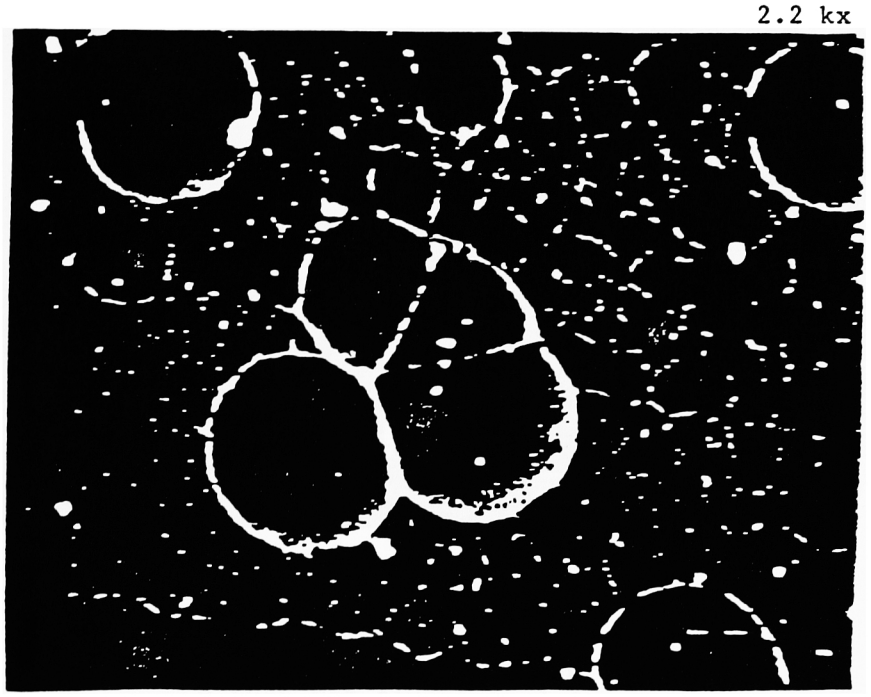

Figure 25. SEM micrographs of Kapton H that was fluorinated for 30 minutes and then etch for 50 minutes.

Figure 26. SEM micrograph of Kapton H that was fluorinated for 30 minutes and then etched for 30 minutes.

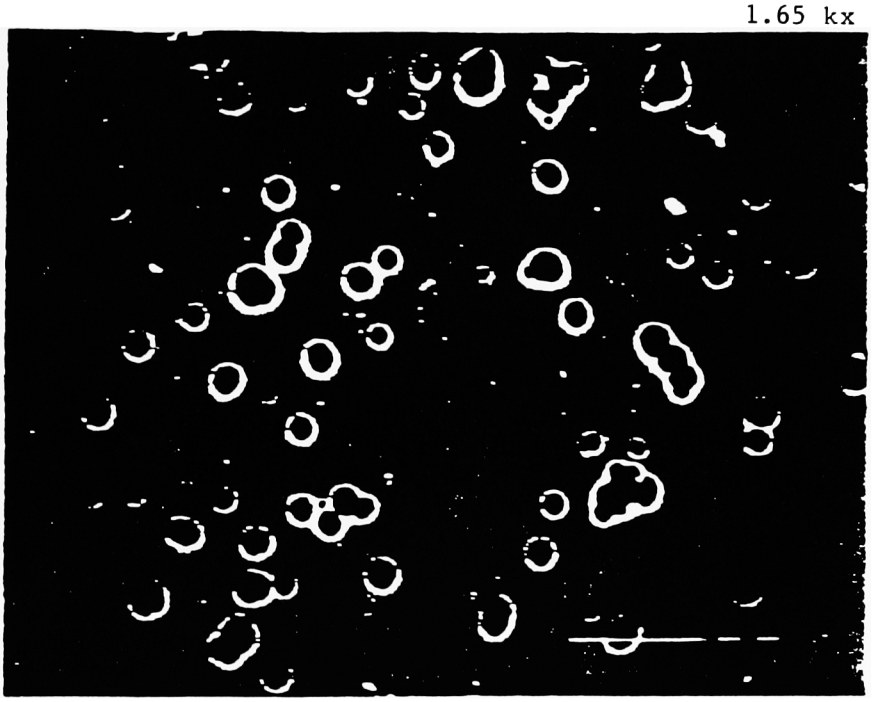

Figure 27. SEM micrograph of Kapton H that was fluorinated for 40 minutes and then etched for 30 minutes.

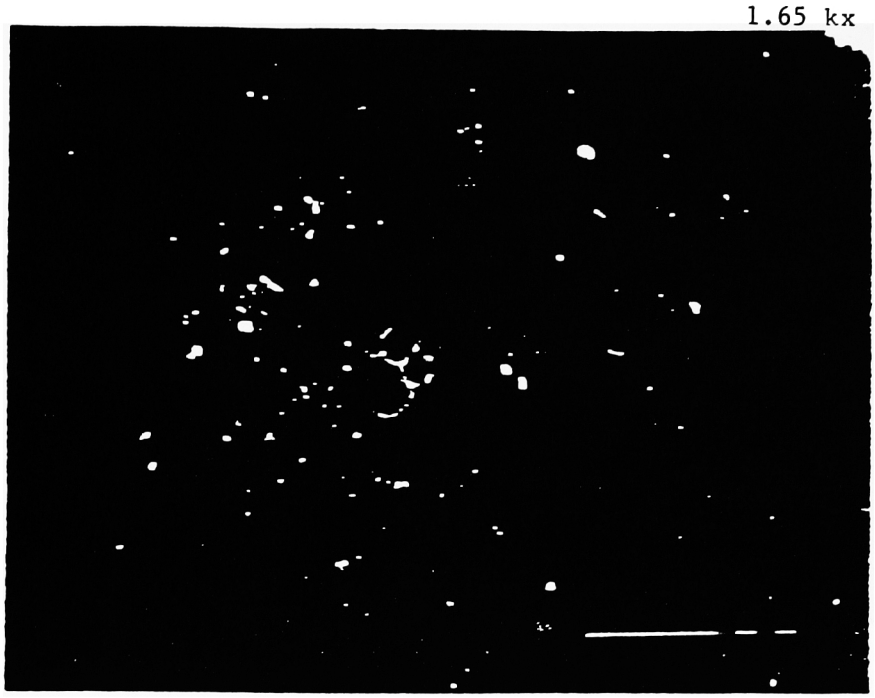

Figure 28. SEM micrograph of Kapton H that was fluorinated for 50 minutes and then etched for 30 minutes.

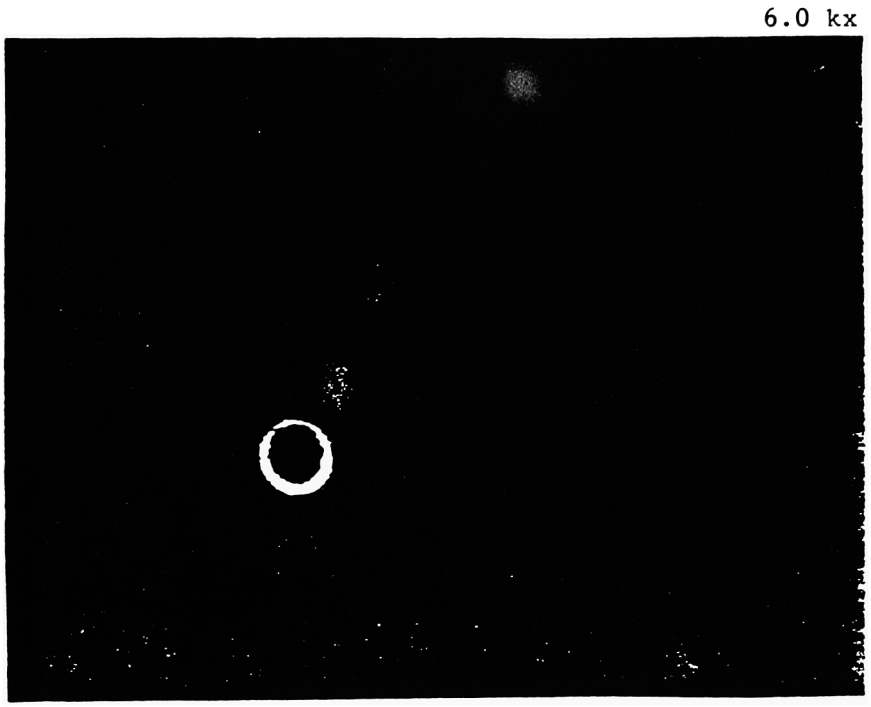

Figure 29. SEM micrograph of Kapton H that was fluorinated for 60 minutes and then etched for 30 minutes.

Table 8

Hole diameters of Kapton H samples that were fluorinated for 30 minutes and then etched for various times.

Fig. No.	Time of Etching [min.]	Hole Diameters [micrometers]	Remarks
22	10	1.2 - 1.9	
23	20	2.0 - 2.5	
24	30	4.0 - 5.0	
25	50	11.0	fluorinated layer is probably etched away.

micrographs are given in Figures 26 to 29 and the diameters of the holes are given in Table 9.

Micrographs 1-7 correspond to Figures 30-36. These micrographs were taken at different locations on a spin coated PI sample that was fluorinated for 60 minutes and then etched for 30 minutes. The location of the micrographs are shown in Figure 37. The diameters of the holes are given in Table 10.

Figure 38 is an edge-on view (Figures 14a and 14b) of a spin coated PI sample that was fluorinated for 30 minutes and then etched for 60 minutes. This view provided a depth profile of the holes formed during the removal of the passivated layer. The average hole depth was 3.8 ± 0.5 micrometers and the average width was 6.7 ± 0.7 micrometers

Table 11 is the magnification coding system that was used to determine the depth and width of the holes.

4.0 DISCUSSION

4.1 Discussion of the Etching Experiments

PI and PS had the lowest etch rate maxima (Figure 16). This is in good agreement with other papers [4,5] that observed aromatic polymers to be more resistant to etching than saturated or unsaturated polymers. Both PI and PS

Table 9

Hole diameters of Kapton H samples that were fluorinated for various times and then etched for 30 minutes.

Fig. No.	Time of Previous Fluorination [min.]	Hole Diameters [micrometers]
26	30	1.7 - 4.6
27	40	1.7 - 2.3
28	50	0.9 - 1.7
29	60	0.9

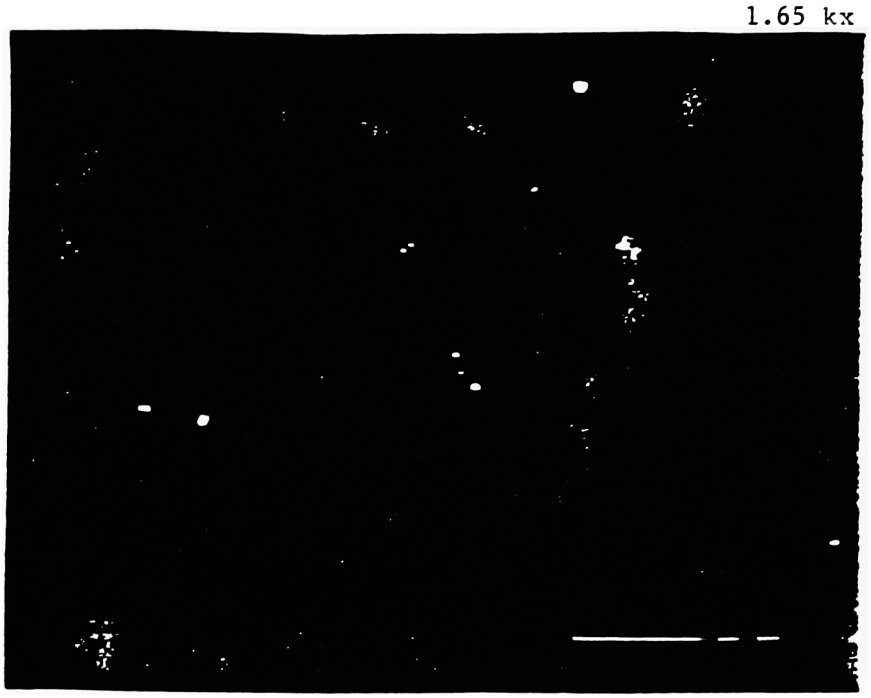

Figure 30. SEM micrograph #1 of a spin coated PI wafer that was fluorinated for 60 minutes and then etched for 30 minutes.

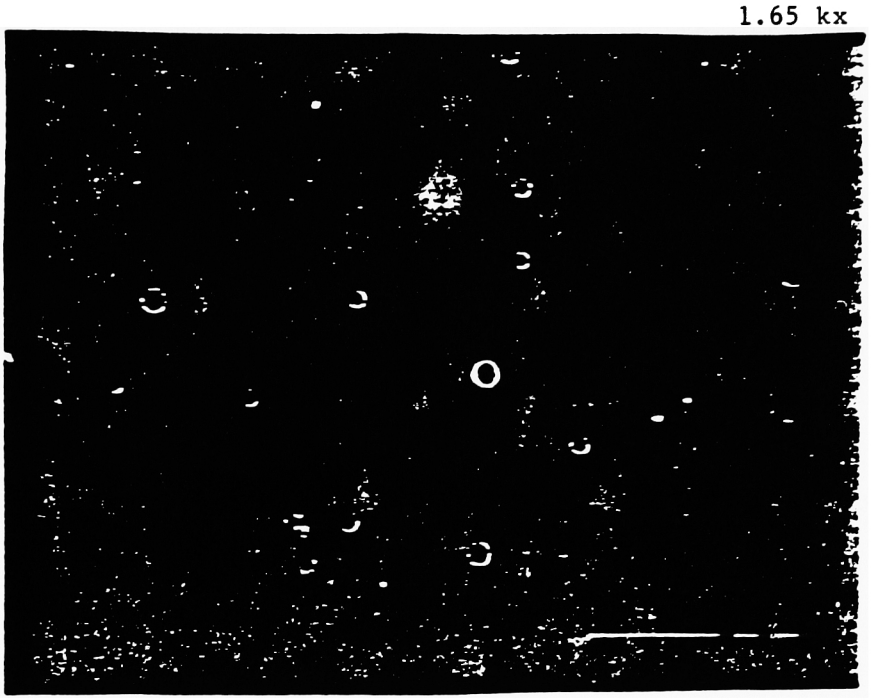

Figure 31. SEM micrograph #2 of a spin coated PI wafer that was fluorinated for 60 minutes and then etched for 30 minutes.

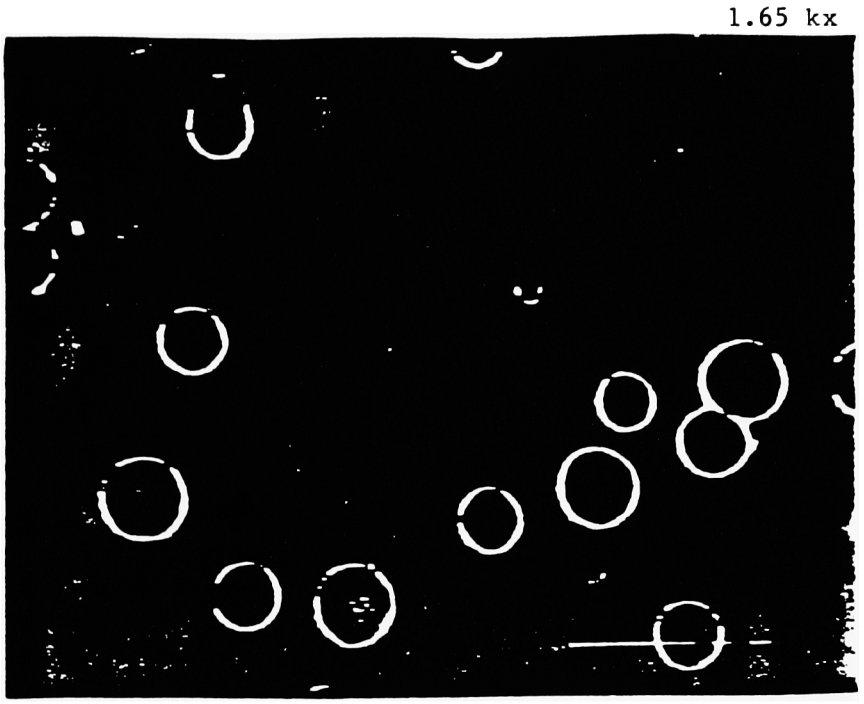

Figure 32. SEM micrograph #3 of a spin coated PI wafer that was fluorinated for 60 minutes and then etched for 30 minutes.

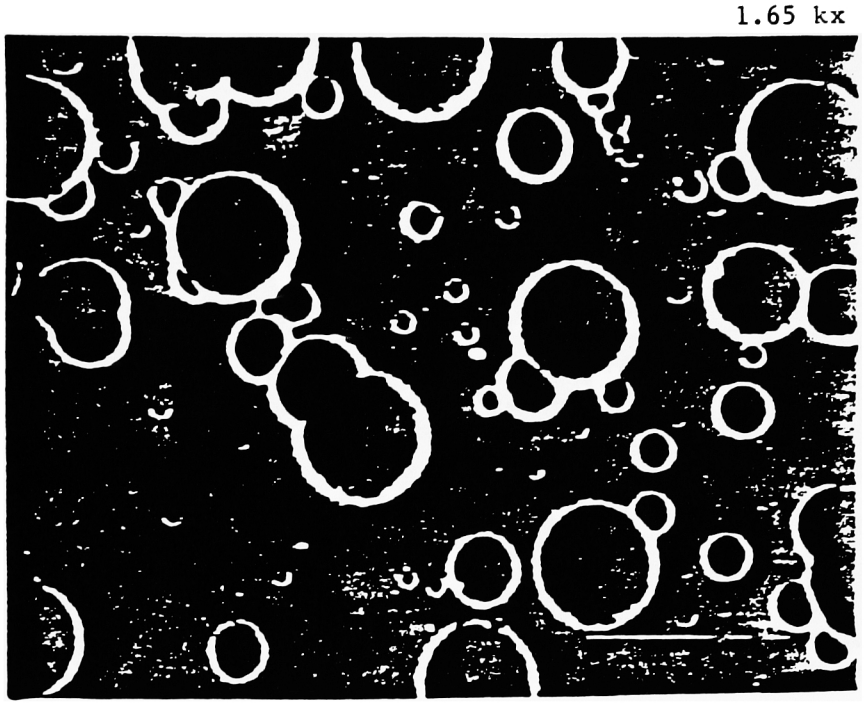

Figure 33. SEM micrograph #4 of a spin coated PI wafer that was fluorinated for 60 minutes and then etched for 30 minutes.

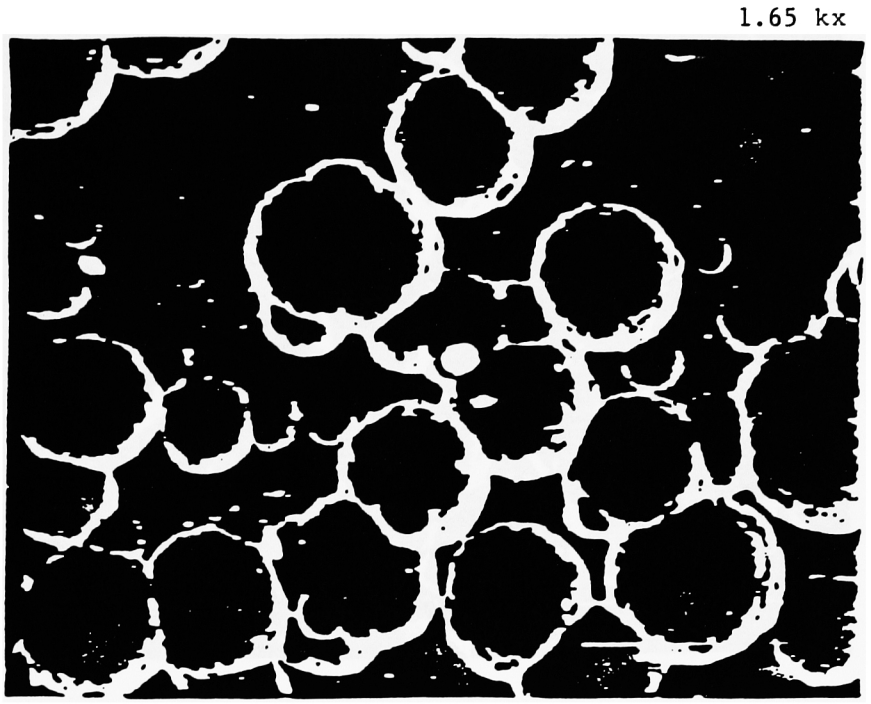

Figure 34. SEM micrograph #5 of a spin coated PI wafer that was fluorinated for 60 minutes and then etched for 30 minutes.

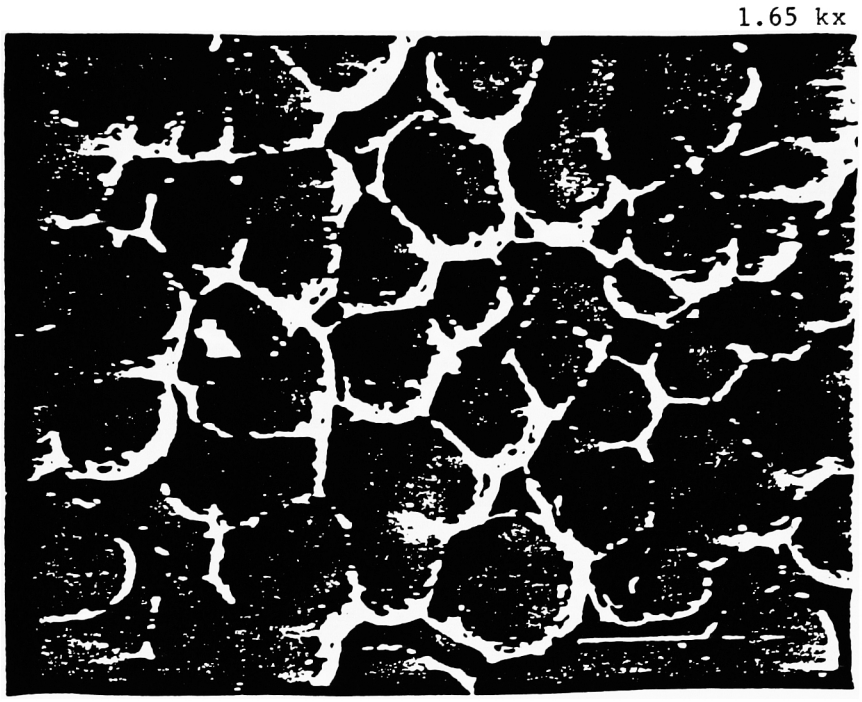

Figure 35. SEM micrograph #6 of a spin coated PI wafer that was fluorinated for 60 minutes and then etched for 30 minutes.

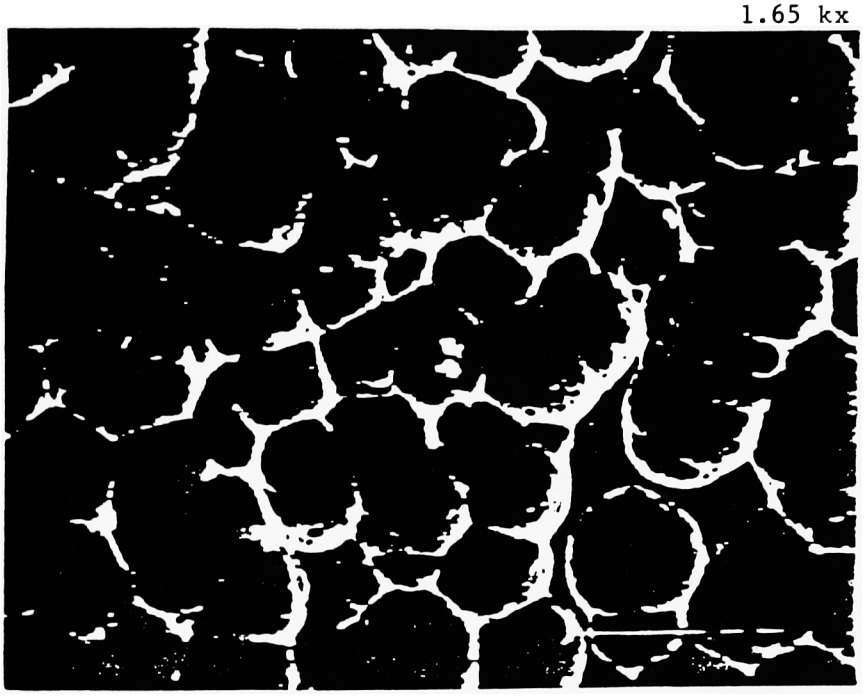

Figure 36. SEM micrograph #7 of a spin coated PI wafer that was fluorinated for 60 minutes and then etched for 30 minutes.

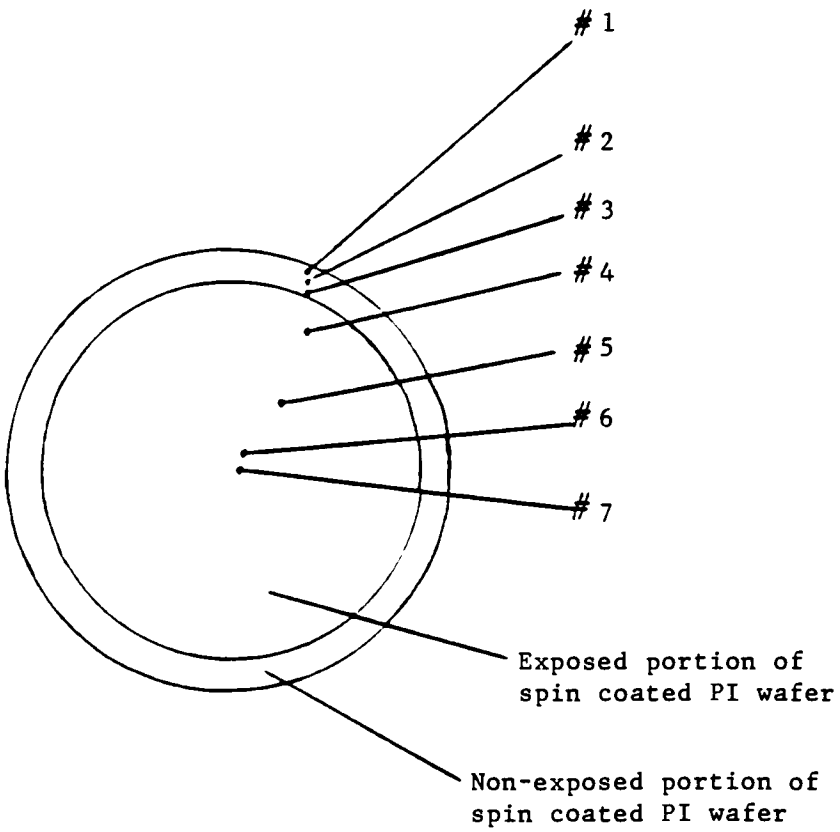

Figure 37. Location of micrographs #1 - #7.

Table 10

Hole diameters at various locations on a spin coated polyimide sample that was fluorinated for 60 minutes and then etched for 30 minutes.

Fig. No.	Micrograph No.	Hole Diameters [micrometers]
30	1	0.65 - 1.0
31	2	1.0 - 1.7
32	3	1.7 - 6.0
33	4	1.0 - 10.0
34	5	10.0
35	6	10.0
36	7	10.0

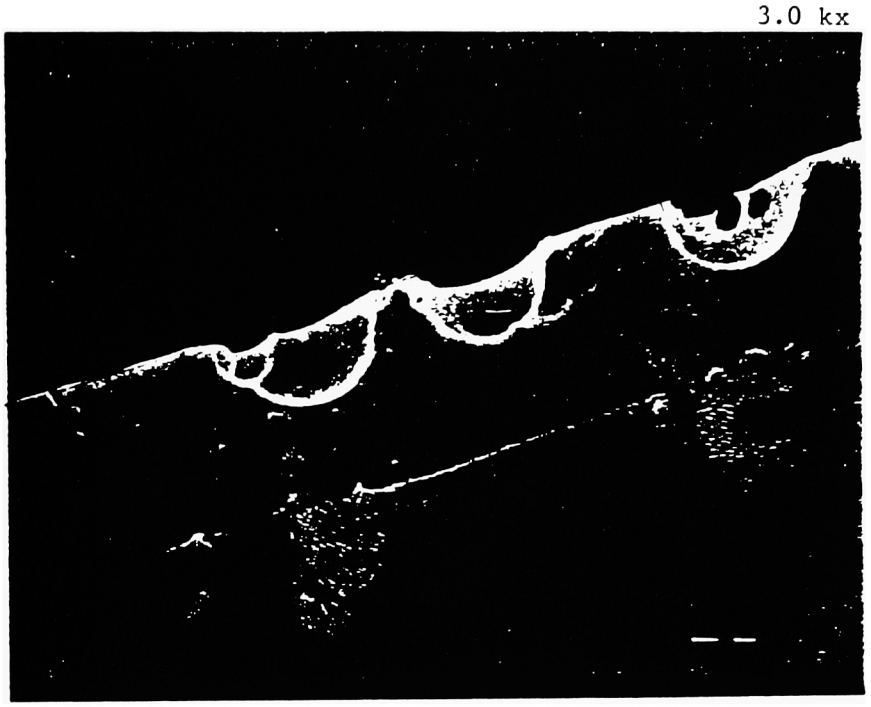

Figure 38. Edge-on view of a spin coated PI wafer that was fluorinated for 30 minutes and then etched for 60 minutes.

Table 11

Magnification Coding System For the ISI-40 Scanning Electron Microscope.

ubar - micrometer bar

The ubar represents:
1. 100 um when followed by three dashes — - - -
2. 10 um when followed by two dashes — - -
3. 1 um when followed by one dash — -
4. 0.1 um when followed by no dashes —

Magnification can be calculated from the ubar by using the following relationships:

10X = 1 mm when the ubar represents 100 micrometers
100X = 1 mm when the ubar represents 10 micrometers
1000X = 1 mm when the ubar represents 1 micrometer
10000X = 1 mm when the ubar represents 0.1 micrometers

A simple formula to quickly calculate the magnification is:

Magnification = (Length of the ubar [mm] x 10^4)/10^n

(n = the number of dashes)

achieved their maximum etch rate at about 85% O2, 10% CF4 and 5% Ar. PB, an unsaturated polymer, achieved a maximum etch rate (75% O2) which was more than 5 times greater than PI and twice as great as PS's maximum etch rate (Figure 16). PE, which is completely saturated, achieved its maximum etch rate at 70% O2 and had a slightly lower maximum etch rate than PB. PVA, which is also saturated, had the highest maximum etch rate; it occurred at 50% O2.

Table 12 compares these results with earlier results (Figure 39) obtained in this laboratory. For the two studies, the gas composition required to reach the maximum etch rate are in good agreement. Although the etch rate curves in Figures 16 and 39 differ for PVA, the general trends of the graphs are similar. The primary distinction between PVA and the other polymers is that the maximum for the etch rate curve is displaced towards lower O2 concentrations.

According to Cain, Egitto and Emmi [6], the amount (number density) of F atoms in the plasma needed to achieve a maximum etch rate is higher for saturated polymers than for unsaturated polymers. The difference in the maxima for saturated and unsaturated polymers can be attributed to the differences in their molecular orbitals. Saturated polymers have a very large gap between the highest occupied (HOMO) and the lowest unoccupied molecular orbital (LUMO) (Figure 40). The theory [16] states that because of this, F atoms have a rather repulsive trajectory when approaching the

Table 12

Comparison of the maximum etch rates, ER, for structurally different polymers.

Max. ER (Å/min)	%O2	Polymer	Max. ER (Å/min)	%O2
3900	85	PI	6367	85.0-81.8
9900	85	PS	19712	79.9
21000	75	PB	17831	78.9-75.9
17500	70	PE	17078	72.0
35000	50	PVA	32858	65.6

Note: The data on the left was collected by the author. The data on the right are previous results obtained by the RIT Plasma Laboratory.

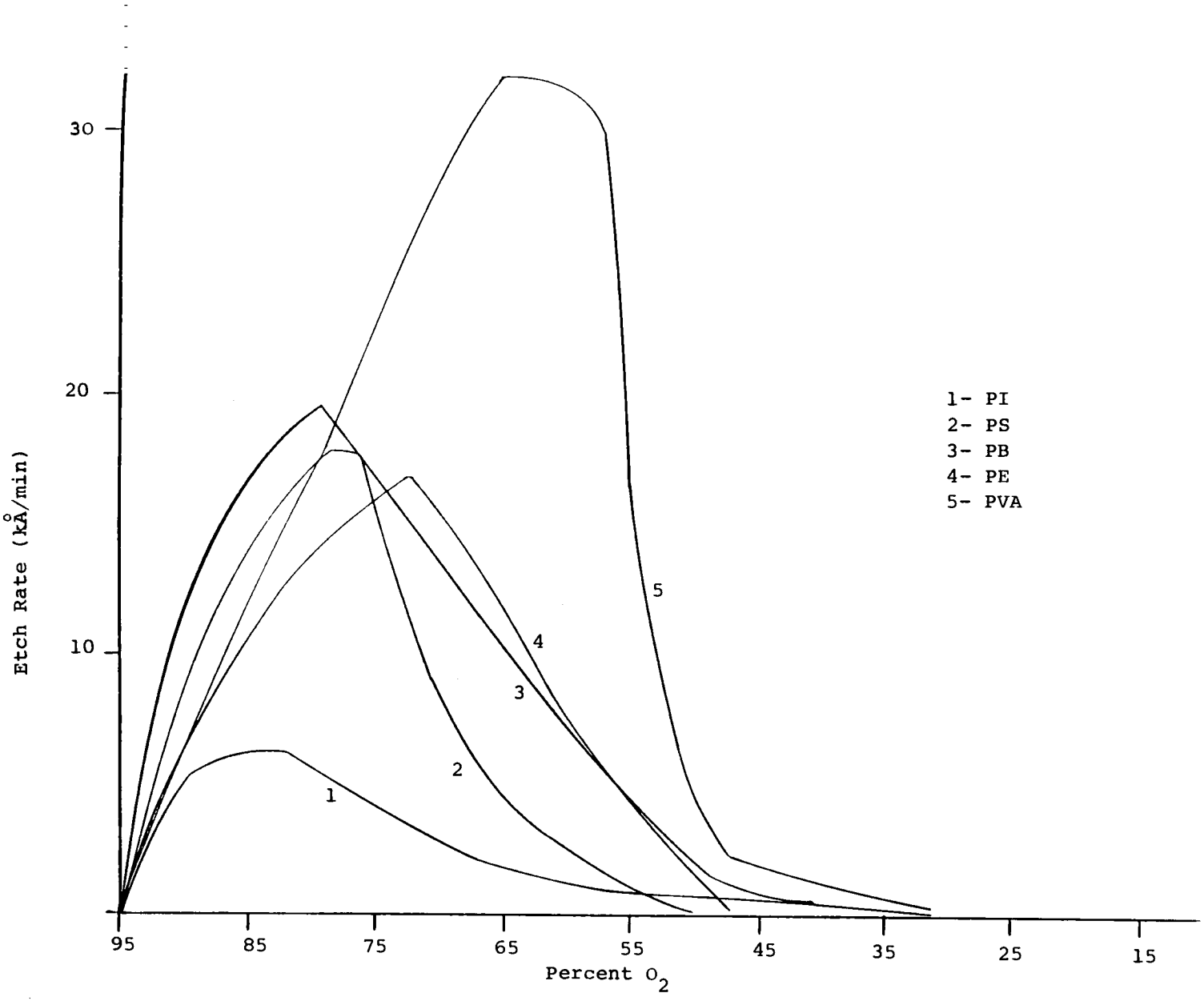

Figure 39. Etch rate of structurally different polymers that were exposed downstream of an O_2-CF_4-Ar microwave plasma.

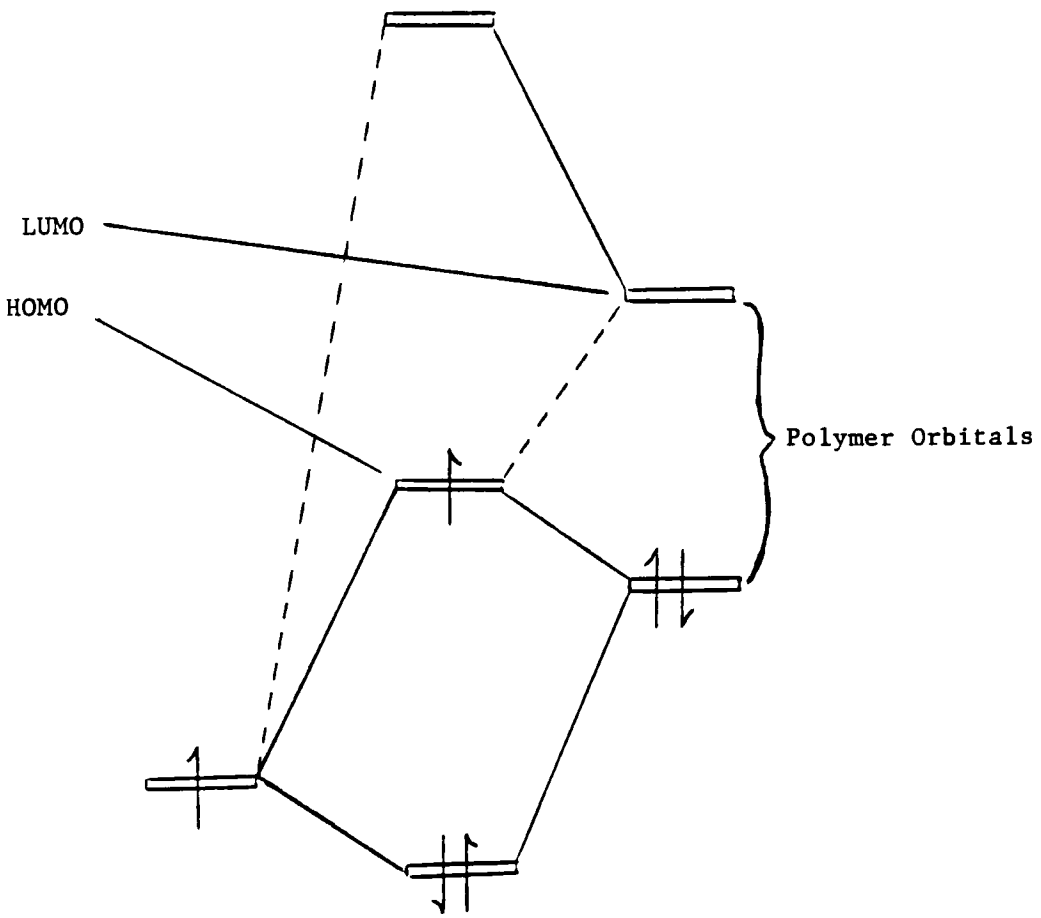

Figure 40. Schematic of a polymer molecular orbital which shows the lowest unoccupied molecular orbital (LUMO) and the highest occupied molecular orbital (HOMO).

reaction zone (zone where chemistry occurs) of a saturated polymer. Since the approach of atomic fluorine to the surface is difficult, it must be present in higher concentrations in order to penetrate the reaction zone. For unsaturated polymers the gap between the HOMO and the LUMO is much smaller than that of saturated polymers. Therefore, a smaller amount of atomic fluorine is needed in order to achieve an etch rate maximum.

In agreement with the above stated model, Wrobel, Lamontagne and Wertheimer [38] found that the percent of CF4 in the gas feed decreases with increasing unsaturation of the polymer's structure. It was also found that the percent of CF4 needed in order to achieve a maximum etch rate, for a given polymer, is about 1.7 times greater for a 13.56 MHz rf generated plasma than for a 2.45 GHz microwave generated plasma. That is, compared to a polymer that is exposed directly to a microwave generated plasma, a polymer that is exposed directly to an rf generated plasma needs approximately 1.7 times more CF4 in the gas feed in order to achieve a maximum etch rate.

The difference in the percent of CF4 in the gas feed has been attributed to the differences in the plasmas' EEDF (electron energy distribution function); the EEDF of a microwave generated plasma being greater than that of an rf generated plasma. This work also concluded that there is a correlation between polymer structure and the activation energy for etching. For instance, the presence of N atoms in

a polymer chain raises the activation energy, whereas materials with oxygen atoms have a low activation energy.

The work of Wrobel et al [38] is summarized and appears in Figure 41. Also shown in Figure 41 is the work of the author, Vukanovic et al [18], Heidenreich, Paraczczak, Moisan and Sauve [39] and Brasseur, Meynen, Degeyter, Verdonck and Coopmans. [40] The figure is a plot of optimum CF4 concentration (%) in a microwave plasma vs. the number of C=C bonds per "mer" mass of the polymer being etched. Wrobel et al [38] etched polyimide, polyamide (PA), polyethylene terephthalate (PET), poylcarbonate (PC) and epoxy resin (ER) in a 2.45 GHz microwave plasma. The author etched PI, PS, PB, PVA and PE downstream of a 2.45 GHz microwave plasma. Vukanovic et al [18] etched PI downstream of a 2.45 GHz microwave plasma. Heidenreich et al [39] etched polymethyl-methacrylate (PMMA) downstream of a 915 MHz microwave plasma. Brasseur et al [40] etched HPR-204 (a novolak-based photoresist) downstream of a 2.45 GHz microwave plasma.

The trend of the graph shows that the percentage of CF4 that is needed to achieve a maximum etch rate decreases with increasing degree of unsaturation; regardless of where the polymers are in relation to the plasma. The downward slope of the graph holds true for the polymers that were etched downstream of the plasma and for the polymers that were etched in the plasma. This suggests that neutral chemistry plays an important role in the etching process.

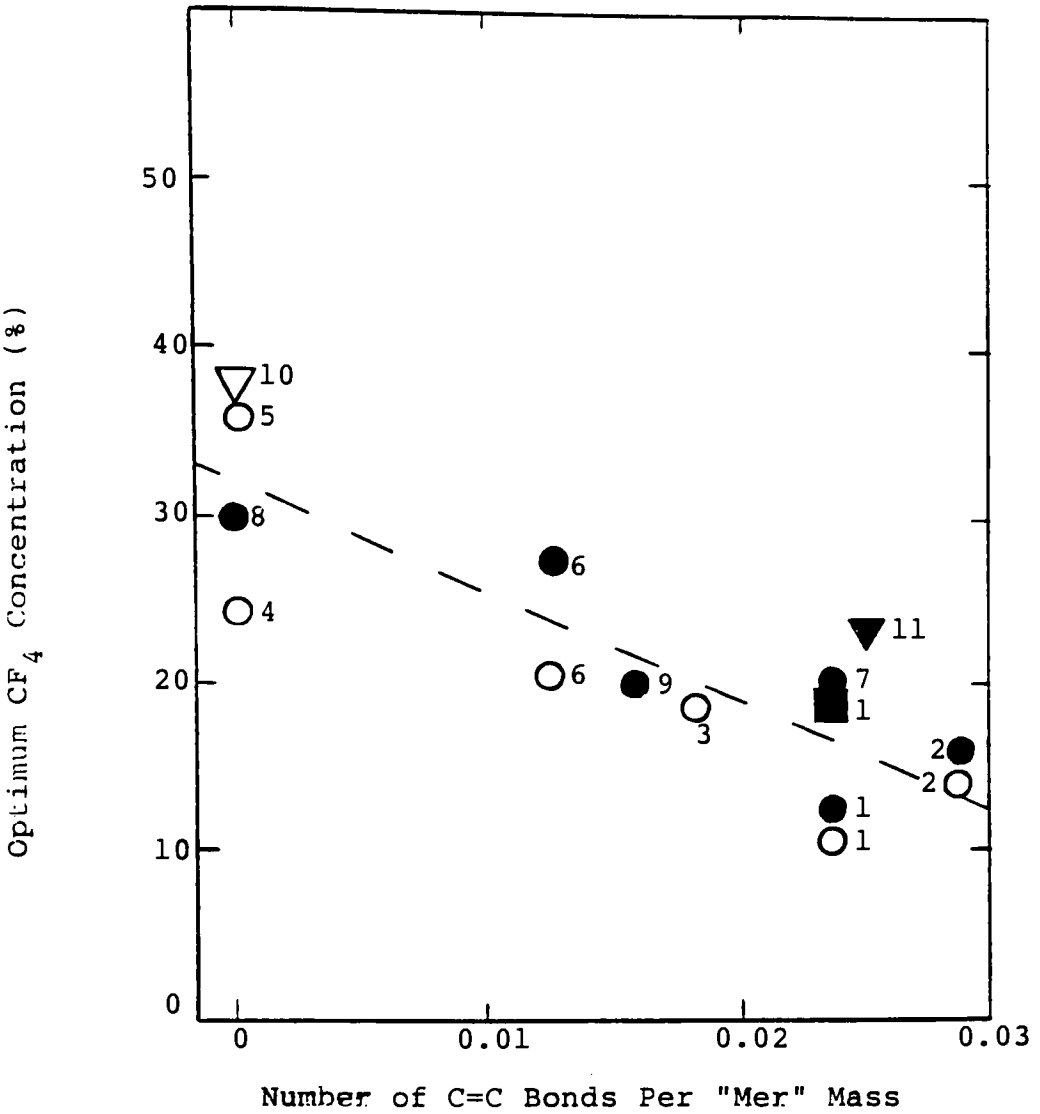

Figure 42. Optimum concentration of CF_4 in a microwave plasma vs. the number of C=C bonds per "mer" mass. Closed circles [38], Open circles this work, Closed triangle [40], Open triangle [39], Closed square [18].
(1) PI, (2) PS, (3) PB, (4) PE, (5) PVA, (6) EP, (7) PC, (8) PA, (9) PET, (10) PMMA, (11) HPR-204.

The earlier work of Matuszak [23] differs from the author's work in that Matuszak reported values of 75% O2, 20% CF4 and 5% Ar for the composition of gases that yielded the maximum etch rate for spin coated polyimide samples. I found values of 85% O2, 10% CF4 and 5% Ar. The work of Matuszak and myself was performed using essentially the same equipment. I offer three reasons for the difference: 1) the condition of the etching system (eg. the chamber walls) is subject to change over a period of a few years, 2) Matuszak used a pyrex injector tube and I used a quartz injector tube and 3) my samples were closer to the plasma. I want to reemphasize, however, that it is not the percentage of O2 in the gas feed that determimes etch rate maximums; it is the [O]/[F] ratio.

4.2 Discussion of the Fluorination Experiments

All the polymers (PS,PVA,PE and Kapton H) achieved their maximum contact angles in the 20% - 5% oxygen range. This also corresponds to a maximum in the ratio of atomic line intensities of IF/IAr (Figure 13). This suggests that the polymers tested became more teflon-like when there was a maximum in the F atom concentration of the plasma. Contact angle measurements done in this lab yielded a value of 108 degrees for Teflon.

Table 4 shows the contact angles of the polymers before and after they were exposed to a F-rich plasma. The aromatic polymers (PI and PS) exhibited the least amount of change between their maximum contact angle and their contact angle before fluorination. The percent difference in contact angle between the aromatic polymers and the saturated (PE and PVA) was over twice as great. For example, the percent difference for PVA was 55 and the percent difference for PI was 20.2.

4.3 Discussion of the Removal of Passivation Experiments

The removal of the plasma-fluorinated layer was accomplished by exposing the polymers downstream of an O-rich MW plasma. Figure 42 is an interferogram of the transition from slow to fast etching as the surface changes from a fluorinated to an oxygenated layer.

Figure 18 shows a nearly linear time dependency between the time of fluorination of PI samples and the time of removal of the fluorinated layer (Refer 3.3). Samples A, B and C were fluorinated for 20, 46 and 120 minutes, respectively. The fluorinated layer is removed when the resumption of fast etching begins. The time to remove the fluorinated layers from samples A, B and C was 30, 59 and 145 minutes respectively.

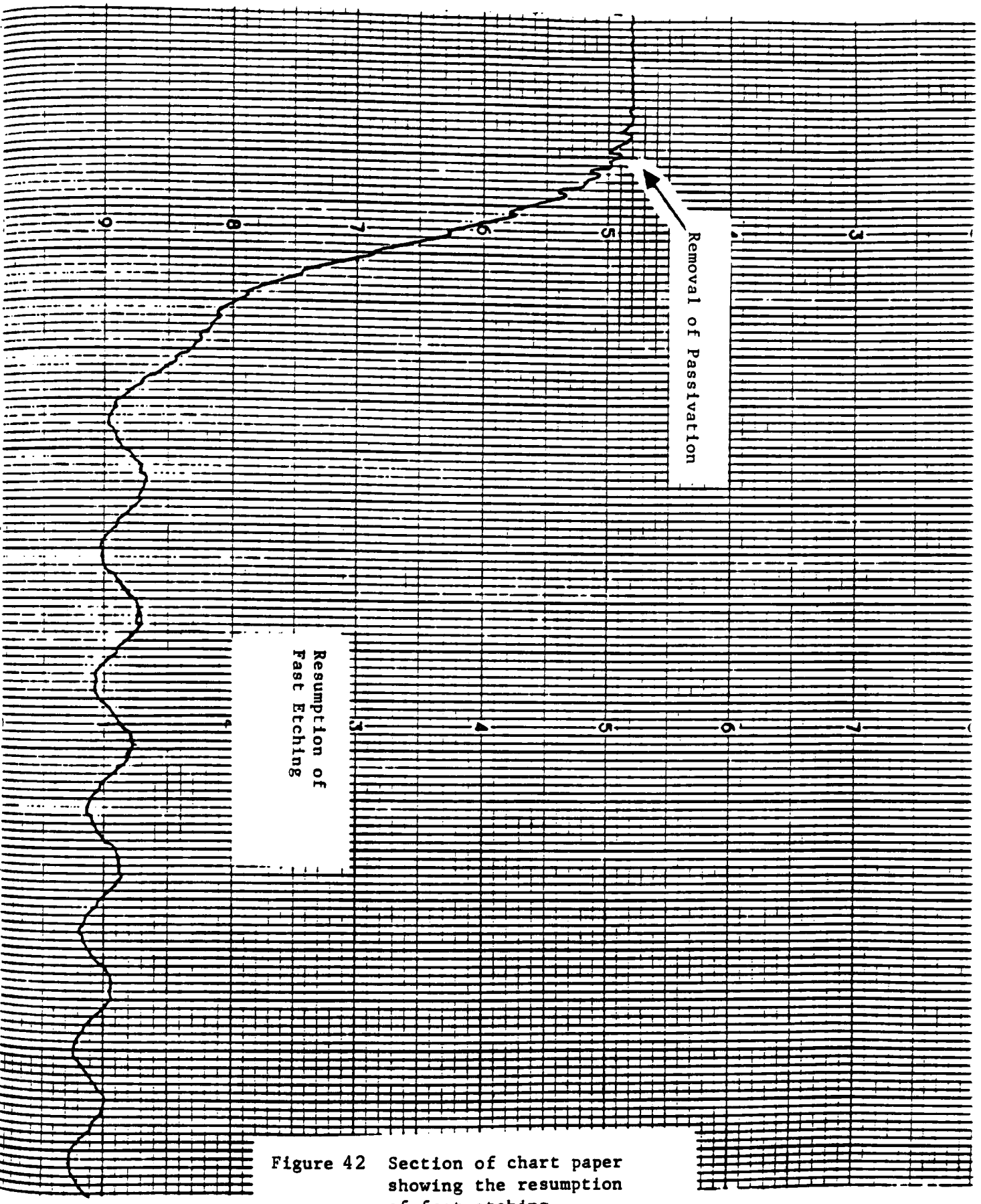

Figure 42 Section of chart paper showing the resumption of fast etching

Figure 19 is the graph of weight loss of PI samples that were fluorinated for different times vs. time of exposure to the O-rich plasma. The sample that was fluorinated for the longest time (60 min.) lost the least amount of weight. Conversely, the greatest weight loss occurred for the sample that was fluorinated for the least time (20 min.).

During the removal of passivation process (ROP), at least two processes are occurring downstream of the MW plasma: 1) the slow removal of the fluorinated layer, which can be detected by laser interferometry and 2) the etching of PI beneath the fluorinated layer, which can not be detected by laser interferometry. The etching of PI beneath the fluorinated layer was detected by gravimetric measurements. Process 2 is believed to occur either by: 1) the diffusion of active species, probably O atoms and F atoms, through the fluorinated layer and reaction products in the opposite direction or 2) the etching of non-modified PI through holes in the fluorinated layer which develop during the ROP process. [41] The latter case is the most likely explanation.

During etching beneath the fluorinated layer, the "corresponding thickness" enables a comparison to be made with the etching of non-fluorinated substrates. It is probably not a direct measurement of the thickness change of a fluorinated substrate. [42]

By use of the "corresponding thickness" equation, the weight loss per unit time data of Figure 19 was converted into thickness loss per unit time. This thickness loss per unit time is known as the "corresponding etch rate". The results of the conversion are shown in Figure 20.

Curve 1 (Figure 20) is the etching of non-fluorinated PI (measured by laser interferometry). Curve 2, which represents a PI sample that was fluorinated for the least amount of time (20 min.) achieved the highest "corresponding etch rate". Curve 5, which represents a PI sample that was fluorinated for 60 minutes, had the lowest "corresponding etch rate".

4.4 Discussion of the Scanning Electron Microscope Investigations

Fluorination does not change the initially smooth surface of the Kapton H film (Figure 2). However, holes appear on the surface of samples that have been exposed to an O-rich plasma. There is a difference, in the appearance of the holes, between fluorinated and non-fluorinated samples. Without fluorination, the holes are shallow and the bottom of the holes can be seen (Figure 21). With fluorination the holes are much deeper and the bottom of them can not be observed.

The fluorinated layer is probably not completely etched away in Figure 24 because of the presence of holes with no observalable bottoms. The layer is likely to be gone in Figure 25 owing to the observation of shallow bottomed holes. The diameters of the holes in Figures 22-24 increased as the time of exposure to the O-rich plasma increased (Table 8).

Table 9 shows that as the time of fluorination of a Kapton H sample increases, the diameters of the holes formed during the ROP process decrease.

The diameters of the holes of a spin coated PI sample that was first fluorinated for 60 minutes then etched for 30 minutes is shown in Table 10. The diameters decreased going from the center of the sample to its periphery. The center of the sample, because of the geometry of the reactor chamber, is subjected to a greater density of plasma produced gas species. This is the best reason as to why one observes greater hole diameters at the center of the sample.

Four holes with an average depth of 3.8 + 0.5 micrometers can be seen in Figure 37. The average width of the holes is 6.7 + 0.7 micrometers. The void in the hole wall the upper right of Figure 37 suggests that two, or possibly more holes, are converging on one another. As the hole diameters increase, there is a point in time at which all of the holes "engulf" one another.

5.0 CONCLUSION

Investigations of the etching, passivation and the removal of passivation of structurally different polymers in the absence of ions, photons and electrons was accomplished by studying the polymers downstream of a microwave plasma.

The percent of molecular oxygen in the gas feed that produced a maximum etch rate varied for the different polymers. Compared to unsaturated polymers, saturated polymers require less O2 and more CF4 in their gas feed in order to achieve a maximum etch rate. Aromatic polymers are the most resistant to the etching process.

Fluorination of the polymers occurred when they were exposed downstream of a MW plasma that contained high concentrations of CF4 in the gas feed. An increase in the contact angle of the polymers was observed when they were exposed to high F-rich plasmas. The polymers achieved their highest contact angles when the plasma contained between 75%-90% CF4. This range corresponds to the range at which the IF/IAr ratio is at a maximum. This suggests that the polymers became more teflon-like when the F atom concentration in the plasma is at a maximum. Contact angle measurements were taken before and after exposure to the F-rich plasma. The aromatic polymers exhibited the least percent change in their contact angles.

Exposure of plasma-fluorinated PI and Kapton H downstream of an O-rich plasma resulted in the removal of the passivated layer. The passivated layer is removed when the resumption of etching is observed. The time needed to remove the passivated layer was roughly equivalent to the time of passivation. Small holes developed in the plasma-fluorinated layer during the removal of passivation (ROP) process.

Kapton H was fluorinated for various times and the time of removal was held constant. As the fluorination time increased, the hole diameters decreased. In another experiment, fluorination times were held constant and the ROP times were varied. For this experiment, the hole diameters increased with increased ROP times.

By use of the "corresponding thickness" equation, a change in weight loss was converted to a change in thickness loss. During the ROP process, gravimetric analysis showed a greater thickness loss of PI than did laser interferometry. The holes in the fluorinated layer, formed during the ROP process, allowed the reactive gas species to etch the non-modified PI beneath the fluorinated layer. Etching beneath the fluorinated layer can not be detected by laser interferometry.

REFERENCES

1. F. Emmi, F. Egitto, V. Vukanovic and R. Horwath Proceed. Fifth Sym. on Plasma Proceed., Electrochem. Soc. Fall Meeting, (1984).

2. F. Egitto, F. Emmi, R. Horwath and V. Vukanovic, J.Vac. Sci. and Technol., B3 (3) 893, 1985.

3. J. W. Coburn, Plasma Chem. and Plasma Proc., 2, p. 15 (1982).

4. R. H. Hansen, J.V. Pascale, T. De Benedictics and P.M. Rentzepis, J. Poly. Sci.: Part A, 3, p.2205 (1965).

5. G. N. Taylor and T. M. Wolf, Polyer Eng. and Sci., 20, 16, (1980).

6. S. R. Cain, F. Egitto and F. Emmi, J. Vac. Sci. and Technol., A5 (4), p. 1583 (1987).

7. D. L. Flamm amd V. M. Donnelly, Plasma Chem. and Plasma Proc., 1, 317 (1981).

8. J. F. Rembetski, M.S. Dissertation, Dept. of Chem. Eng., Clarkson University, (1985).

9. J. A. Kerr and S. J. Moss (eds.), Handbook of Biomolecular and Termolecular Gas Reactions, 1, CRC Press. (1981).

10. H. J. Leary Jr. and D. S. Campbell, Photon, Electron and Ion Probes of Polymer Structure and Properties, edited by D. W. Wright, T. J. Fabish and H. R. Thomas. ACS Sym. Series, 162 (1981).

11. J. Dedinas, M. Feldman, M. Mason and L. Gerenser, Internat. Conf. of Plasma Chem. and Tech., ed. by Herman Boenig, p. 119, (1983).

12. J. W. Coburn, "Plasma Etching", Integrated Circuit Tech. for the 1980's (Continuing Education, U.C. Berkley), Feb. 1980.

13. C. J. Mogab, J. Electrochem. Soc., 124, 8,(1977).

14. J. W. Coburn and H. F. Winters, J. App. Phys., 50, 5 (1980).

15. Y. Horiike and M. Shibagaki, Electrochem. Soc. Softbound Proceed., p.1073 (1977).

16. S. J. Fonash, Solid State Technol., p. 150, 1985.

17. F. Egitto V. Vukanovic and G. Taylor. "Plasma Etching of Organic Polymers", to be published.

18. V. Vukanovic, G. Takacs, E. Matuszak, F. Egitto, F. Emmi and R. Horwath, J. Vac Sci. Tech., B6 (1), 66 1988.

19. V. Vukanovic, G. Takacs, E. Matuszak, F. Egitto, F. Emmi and R. Horwath, J. Vac. Sci. Technol., A4,(3), 698, (1986).

20. J. Dedinas, M. Feldman, M. Mason and L. Gerenser, Second Int. Conf. of Plasma Chem. and Tech., San Diego, CA., Nov., p. 250, 1984.

21. M. Anand. R. E. Cohen and R. F. Baddour, "Photon, Electron and Ion Probes of Polymer Structure and Properties", ed. by D.W. Dwight, T. J. Fabish and H. R. Thomas. ACS Symposium Series, 162, p. 353, (1981).

22. L. J. Matienzo, F. Emmi, F. Egitto, D. Van Hart V. Vukanovic and G. Takacs, J. Vac. Sci. Technol. A6 (3), 950, 1988.

23. E. A. Matuszak, M.S. Thesis, Dept. of Chem., Rochester Institute of Tech., (1986).

24. J. M. Cook, J. Hannon and B. Benson, ISPC-6, C-2-2, p.617 (1983).

25. E. Kay, J. Coburn and A. Dilks, "Plasma Chemistry 3", ed. by S. Verprek and M. Venugopalan (Springer, Berlin, 1980), pg. 3.

26. D. L. Flamm, V. Donnelly and D. Ibbotson, J. Vac. Sci. Technol., B1, 23, (1983).

27. C. J. Mogab, A. Adams and D. Flamm, J. App. Phys., 49, p. 3803 (1978).

28. G. K. Vinogradov, P. Nevzorov, L. Polak and D. Slovetsky, Vacuum, 32, p. 1253 (1981).

29. F. Egitto, V. Vukanovic, R. Horwath and F. Emmi ISPC-7, A-3-6, p.986 (1985).

30. Ch. Steinbruchel,B. Curtis, H. Lehmann and R. Widmer IEEE Trans. Plasma Sci., PS-14, 2, pg. 137 (1986).

31. I. C. Plumb and K. R. Ryan, Plasma Chem. and Plasma Proc., 6, 3, (1986).

32. MKS Instruments Operating Instructions; High Accuracy Control Systems for Vacuum-Pressure-Flow, May 1979.

33. Tylan Instrument Manual, Oct. 1984.

34. Dupont, Kapton Catalogue (Summary of Properties), p. 4, 1987.

35. F. W. Billmeyer, "Textbook of Polymer Science", Third Edition, John Wiley and Son, p. 478, 1987.

36. M. Klausner, I. H. Loh, R. F. Baddour and R. E. Cohen Polymeric Materials Sci. and Eng., 56, p. 227, 1987.

37. M. A. Fortes, Physiochem. Aspects Polym. Surf., ed. K. Mittal, 1, p. 108, 1981 (Pub 1983).

38. A. M. Wrobel, B. Lamontagne and M. R. Wertheimer, Plasma Chem. and Process., 8, 315 (1988).

39. J. E. Heidenreich, J. R. Paraszczak, M. Moisan and G. Sauve, J. Vac. Sci. Technol., B5, 347 (1987).

40. G. Brasseur, H. Meynen, P. Degeyter, P. Verdonck and F. Coopmans, 8th Intern. Sym. on Plasma Chem. (ISPC-8), Tokyo, Japan, p. 939 (1987).

41. V. Vukanovic, G. Takacs, E. Matuszak, F. Egitto, F. Emmi and R. Horwath, ISPC-8, C11-02, (1987).

42. Rochester Institute of Technology Report on IBM-SUR Grant, March 1988.